Weak interaction processes on deuterium: Muon capture and neutrino reactions

Naoko Tatara*
Department of Physics, Sophia University, Kioi-cho, Chiyoda-ku, Tokyo 102, Japan

Y. Kohyama
Fuji Research Institute Corporation, 3-2-12, Kaigan, Minato-ku, Tokyo 108, Japan
and Department of Physics, Sophia University, Kioi-cho, Chiyoda-ku, Tokyo 102, Japan

K. Kubodera†
Department of Physics and Astronomy, University of South Carolina, Columbia, South Carolina 29208
and Department of Physics, Sophia University, Kioi-cho, Chiyoda-ku, Tokyo 102, Japan
(Received 22 May 1990)

A detailed calculation of the capture rate for $\mu^- + d \to \nu_\mu + n + n$ is carried out and the result compared with the latest data. Within the same framework we also calculate the cross sections of $\nu + d$ and $\bar{\nu} + d$ reactions for incident energies $E_\nu \leq 170$ MeV in view of the importance of these cross sections for studying astrophysical neutrinos with the use of a heavy-water Čerenkov counter.

I. INTRODUCTION

Studying weak-interaction processes on the deuteron is interesting for multiple reasons. From the nuclear physics point of view, it offers a useful testing ground of our understanding of exchange current effects, for the structure of two-body nuclear systems is known with much better accuracy than that of complex nuclei.[1-5] It is to be recalled here that the most convincing evidence of exchange currents for electromagnetic processes has been obtained through investigations of the reactions $n + p \to \gamma + d$ (Ref. 6) and $e + d \to e + n + p$.[7,8] In the astrophysical context, the detailed knowledge of the cross sections for $p + p \to d + e^+ + \nu_e$ and $p + e^- + p \to d + \nu_e$ is crucially important for the quantitative description of the thermonuclear processes occurring in the Sun.[9] We should further add that a project to build a heavy-water Čerenkov counter for detecting astrophysical neutrinos is in progress.[10] Reasonably reliable estimates of the cross sections for ν-d reactions[11] are a prerequisite for extracting useful astrophysical information from data that would become available from the Sudbury project.[10]

Recently, there was a new measurement[12] of the rate for muon capture by a free deuteron:

$$\mu^- + d \to \nu_\mu + n + n \ . \tag{1}$$

It is known that the μ-d capture takes place practically uniquely from the μd hyperfine doublet state, and the experiment[12] measured λ_d, the total capture rate for the hyperfine doublet state. The reported value is $\lambda_d^{\rm expt} = 470 \pm 29\ {\rm s}^{-1}$, which is significantly larger than any existing theoretical estimates.[1,2] Since, as mentioned above, the structure of the two-body nuclear systems is reasonably well understood, this discrepancy, if really confirmed, should constitute a serious challenge to our understanding of the nuclear response to weak-interaction probes. On the other hand, the latest experimental result[13] indicates that $\lambda_d^{\rm expt} = 409 \pm 40\ {\rm s}^{-1}$, in good agreement with the calculated values given in the literature.[1,2] Expecting further developments in the measurement of $\lambda_d^{\rm expt}$ in the near future, we consider it worthwhile to reexamine the theoretical estimates of λ_d. One of the purposes of this article is to present a new calculation of λ_d, in which various ingredients that go into its estimation are carefully examined.[14]

A detailed study of the μ-d capture is expected to provide a measure of the reliability of our description of intermediate-energy weak-interaction processes in the $A = 2$ nuclear system. This information will be useful when we try to estimate the neutrino-deuteron reaction cross sections. For low incident neutrino energies relevant to the solar neutrinos, the ν-d reaction cross sections were calculated in a number of works,[15-18] the most up-to-date ones given in Ref. 17 for the charged-current reaction and in Ref. 18 for the neutral-current reaction. As is well known, neutrinos produced in more violent processes than the solar thermonuclear reactions can also play important astrophysical roles, and their observation provides us with valuable information. A dramatic example is the detection of the supernova neutrinos by the Kamiokande group[19] and by the IMB group.[20] Since the Sudbury heavy-water Čerenkov counter can be used also for detecting these higher-energy neutrinos, it would be of great current interest to provide reliable estimates of the ν-d and $\bar{\nu}$-d reaction cross sections for higher energies than hitherto available. A second purpose of this article is to estimate the cross sections for ν-d and $\bar{\nu}$-d reactions for medium energies ($E_\nu \leq 170$ MeV),[45] using the framework that has been tested with the μ-d capture. We will try here to improve the estimates given in Refs. 17 and 18.

The organization of the paper is as follows. Sections II and III are concerned with the capture rate for $\mu^- + d \to \nu_\mu + n + n$. After describing the formalism in Sec. II, we present the numerical results in Sec. III. We then proceed to evaluate in Sec. IV the cross sections for $\nu + d$ and $\bar{\nu} + d$ reactions. Finally, summary and discussion are given in Sec. V.

II. CAPTURE RATE FOR $\mu^- + d \to \nu_\mu + n + n$

In order to shed more light on the aforementioned controversy on the apparent discrepancy between λ_d^{expt} reported in Ref. 12 and λ_d^{theor}, a systematic examination of the ingredients that go into the existing theoretical treatments will be useful. We wish to make such an examination here. Although the capture rate λ_q for the μd hyperfine quadruplet state can be discussed in the same framework, we will concentrate here on the μd hyperfine doublet capture rate λ_d. Figure 1 depicts the kinematics of the reaction.

The theoretical capture rate of reaction Eq. (1) involves the following three categories of "input" information: (i) the single-nucleon weak-interaction form factors appearing in transition matrix elements for the elementary process $\mu^- + p \to \nu_\mu + n$, (ii) the wave functions of the initial and final two-body nuclear systems, and (iii) the exchange currents. The first systematic study of these features was made by Dautry, Rho, and Riska[1] (DRR) more than a decade ago. Subsequently, Ivanov and Truhlik,[2,21] proposed to use the hard-pion approach in calculating the exchange currents. Comparison of the present work with the previous ones will be made later in the text.

We start with the impulse approximation (IA), neglecting for the moment the exchange-current effects. The weak interaction Hamiltonian H_W is written as

$$H_W = \int d^3x \, \mathcal{H}_W(\mathbf{x}, t=0) , \tag{2}$$

$$\mathcal{H}_W(x) = -\frac{G_F}{\sqrt{2}} \cos\theta_C [J_\lambda(x) L_\lambda(x) + \text{H.c.}] , \tag{3}$$

where the leptonic current is given by

$$L_\lambda(x) = -i \sum_{l=e,\mu,\tau} \bar{\psi}_{\nu_l}(x) \gamma_\lambda (1+\gamma_5) \psi_l(x) , \tag{4}$$

whereas the hadronic current

$$J_\lambda(x) = V_\lambda(x) + A_\lambda(x) \tag{5}$$

has the matrix elements

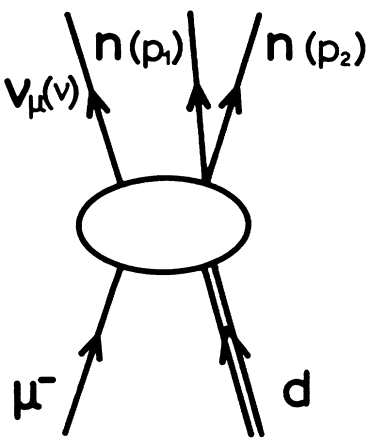

FIG. 1. Kinematics for the $\mu^- + d \to \nu_\mu + n + n$ process.

$$\langle n | V_\mu(0) | p \rangle = i\bar{u}(n)[f_V \gamma_\mu + f_W \sigma_{\mu\nu} k_\nu - i f_S k_\mu] u(p) , \tag{6a}$$

$$\langle n | A_\mu(0) | p \rangle = i\bar{u}(n)[-f_A \gamma_\mu \gamma_5 + i f_P \gamma_5 k_\mu - f_T \sigma_{\mu\nu} k_\nu \gamma_5] u(p) , \tag{6b}$$

where $k \equiv n - p$, with $n(p)$ being the four-momentum of the neutron (proton). The nonrelativistic reduction of the weak-interaction Hamiltonian yields the well-known Fujii-Primakoff effective Hamiltonian[22]

$$H_{\text{eff}} = \tfrac{1}{2} G_F \cos\theta_C \xi_\nu^\dagger (1 - \boldsymbol{\sigma}_l \cdot \hat{\boldsymbol{\nu}}) \times \sum e^{-i\boldsymbol{\nu}\cdot\mathbf{r}_l} \left[F_V + F_A \boldsymbol{\sigma}^{(l)} \cdot \boldsymbol{\sigma}_l - F_P \boldsymbol{\sigma}_l \cdot \hat{\boldsymbol{\nu}} \boldsymbol{\sigma}^{(l)} \cdot \hat{\boldsymbol{\nu}} - \frac{f_V}{m_N} \boldsymbol{\sigma}_l \cdot \hat{\boldsymbol{\nu}} \boldsymbol{\sigma}_l \cdot \mathbf{P}^{(l)} - \frac{f_A}{m_N} \boldsymbol{\sigma}_l \cdot \hat{\boldsymbol{\nu}} \boldsymbol{\sigma}^{(l)} \cdot \mathbf{P}^{(l)} \right] \tau_-^{(l)} \xi_\mu f(\mathbf{x}) , \tag{7}$$

where

$$F_V = \left[1 + \frac{\nu}{2m_N} \right] f_V + m_\mu f_S ,$$

$$F_A = f_A - \frac{\nu}{2m_N} (f_V - 2m_N f_W) , \tag{8}$$

$$F_P = [m_\mu f_P - f_A - (f_V - 2m_N f_W) + 2m_N f_T] \frac{\nu}{2m_N} .$$

Defining the matrix elements of the various terms in the effective Hamiltonian for the initial state $|i\rangle$ and the final state $|f\rangle$ by

$$M_I = \langle f | \sum_{j=1}^{2} \tau_-^{(j)} \exp(-i\boldsymbol{\nu}\cdot\mathbf{x}_j) f(\mathbf{x}_j) \mathcal{O}_I(j) | i \rangle , \tag{9}$$

with $\mathcal{O}_1(i) \equiv 1^{(i)}$, $\mathcal{O}_2(i) \equiv \boldsymbol{\sigma}^{(i)}$, $\mathcal{O}_3(i) \equiv \mathbf{P}^{(i)}$, and $\mathcal{O}_4(i) \equiv \boldsymbol{\sigma}^{(i)} \cdot \mathbf{P}^{(i)}$, the transition amplitude due to the IA contributions can be written as

$$M_{fi} = G_F \cos\theta_C \langle \xi_\nu | \Omega | \xi_\mu \rangle , \tag{10}$$

$$\Omega \equiv \frac{1 - \boldsymbol{\sigma}_l \cdot \hat{\boldsymbol{\nu}}}{2} (\mathcal{M}_1 + \boldsymbol{\sigma}_l \cdot \boldsymbol{\mathcal{M}}_2) , \tag{11}$$

$$\mathcal{M}_1 \equiv F_V M_1 - \frac{f_V}{m_N} (\hat{\boldsymbol{\nu}} \cdot \mathbf{M}_3) , \tag{12}$$

$$\boldsymbol{\mathcal{M}}_2 \equiv F_A \mathbf{M}_2 - F_P \hat{\boldsymbol{\nu}} (\hat{\boldsymbol{\nu}} \cdot \mathbf{M}_2) - i \frac{f_V}{m_N} (\hat{\boldsymbol{\nu}} \times \mathbf{M}_3) - \frac{f_A}{m_N} \hat{\boldsymbol{\nu}} M_4 . \tag{13}$$

In Eq. (10), $|\xi_\mu\rangle$ and $|\xi_\nu\rangle$ represent the lepton spin states.

For the choice of the single-nucleon weak-interaction form factors, the following values will be used as the standard values:[23]

$$f_V(q^2) = 1.0 \times \left[1 + \frac{q^2}{0.71(\text{GeV})^2} \right]^{-2} , \tag{14a}$$

$$f_A(q^2) = -1.262 \times \left[1 + \frac{q^2}{1.19(\text{GeV})^2} \right]^{-2} , \tag{14b}$$

$$2m_N f_W(q^2) = -3.7 \times \left[1 + \frac{q^2}{0.71(\text{GeV})^2}\right]^{-2}, \quad (14c)$$

$$f_P(q^2) = \frac{2m_N}{q^2 + m_\pi^2} f_A(q^2), \quad (14d)$$

$$f_S = 0, \quad (14e)$$

$$f_T = 0. \quad (14f)$$

The value of $f_A(0)$ given in Eq. (14a) has been obtained in a neutron β-decay correlation experiment[23] and is significantly different from the previously accepted value:[24] $f_A(0) = -1.254 \pm 0.006$. The expression for f_P given in Eq. (14d) is based on the partially conserved axial current hypothesis (PCAC) and the Goldberger-Treiman relation. Equations (14e) and (14f) represent the usual ansatz that there is no second-class current. In the present work we also investigate to what extent deviations of the nucleon form factors from the standard values will affect the capture rate.

We next discuss the meson exchange-current (MEC) effects. In Ref. 1, the MEC operators are constructed with the use of the low-energy theorem supplemented by the effective Lagrangian method. Ivanov and Truhlik[21] have derived the MEC in the hard-pion approach, in which one explicitly constructs the effective Lagrangian that is consistent with current algebra, PCAC, and the vector meson dominance. Since the hard-pion approach gives a natural framework in which the soft-pion limit and processes involving finite momentum transfers can be treated on the same footing, we will use here the hard-pion approach.[2,21]

The vertices relevant to our calculation derivable from the effective Lagrangian of Ref. 25 are

$$\mathcal{L}_{\rho\pi\pi} = -g_\rho \boldsymbol{\rho}_\mu \cdot \boldsymbol{\pi} \times \partial_\mu \boldsymbol{\pi}, \quad (15)$$

$$\mathcal{L}_{A_1 A_1 \rho} = g_\rho (\boldsymbol{\rho}_\mu \times \mathbf{a}_\nu - \boldsymbol{\rho}_\nu \times \mathbf{a}_\mu) \cdot \partial_\mu \mathbf{a}_\nu, \quad (16)$$

$$\mathcal{L}_{A_1 \rho \pi} = -\frac{g_{A_1}}{g_\rho f_\pi} \boldsymbol{\rho}_{\mu\nu} \cdot \mathbf{a}_\mu \times \partial_\nu \boldsymbol{\pi} - \frac{1}{4} \frac{g_{A_1}}{g_\rho f_\pi} \left[2 - \frac{g_\rho^2}{g_{A_1}^2}\right] \boldsymbol{\rho}_{\mu\nu} \cdot \boldsymbol{\pi} \times \mathbf{a}_{\mu\nu}, \quad (17)$$

with $\boldsymbol{\rho}_{\mu\nu} = \partial_\mu \boldsymbol{\rho}_\nu - \partial_\nu \boldsymbol{\rho}_\mu$ and $\mathbf{a}_{\mu\nu} = \partial_\mu \mathbf{a}_\nu - \partial_\nu \mathbf{a}_\mu$, where $\boldsymbol{\pi}$, $\boldsymbol{\rho}_\mu$, and $\mathbf{a}_\mu$ are the pion, ρ-meson, and A_1-meson fields, respectively. The effective Lagrangian involving the nucleons can be written as[21]

$$\mathcal{L}_{NA_1\rho\pi} = -\bar{N}\gamma_\mu \partial_\mu N - m_N \bar{N} N - i\tfrac{1}{2} g_\rho \bar{N}\gamma_\mu \boldsymbol{\tau} N \cdot \boldsymbol{\rho}_\mu - i \frac{g_{A_1}}{2 f_\pi} \bar{N}\gamma_\mu \boldsymbol{\tau} N \cdot \boldsymbol{\pi} \times \mathbf{a}_\mu - i \frac{g_{A_1}}{2 f_\pi} \bar{N}\gamma_\mu \gamma_5 \boldsymbol{\tau} N \cdot (\partial_\mu \boldsymbol{\pi} - g_\rho \boldsymbol{\rho}_\mu \times \boldsymbol{\pi}) + i f_A g_{A_1} \bar{N}\gamma_\mu \gamma_5 \boldsymbol{\tau} N \cdot \mathbf{a}_u - \tfrac{1}{4} g_\rho \frac{\kappa_V}{2m_N} \bar{N}\sigma_{\mu\nu} \boldsymbol{\tau} N \cdot \tilde{\rho}'_{\mu\nu}, \quad (18)$$

where

$$\tilde{\rho}'_{\mu\nu} = \boldsymbol{\rho}_{\mu\nu} + \frac{g_{A_1}}{f_\pi g_\rho} (\mathbf{a}_\mu \times \partial_\nu \boldsymbol{\pi} - \mathbf{a}_\nu \times \partial_\mu \boldsymbol{\pi}) + \frac{g_{A_1}}{f_\pi g_\rho} \boldsymbol{\pi} \times \mathbf{a}_{\mu\nu}.$$

Similarly, the part involving the N^* resonance is given by

$$\mathcal{L}_{N^* N A_1 \rho \pi} = 2 \frac{f_{\pi N N^*}}{m_\pi} \bar{N}^*_\nu \mathbf{T} N \cdot \nabla_\nu \boldsymbol{\pi} + g_\rho \frac{G_1}{m_N} \bar{N}^*_\mu \gamma_5 \gamma_\nu \mathbf{T} N \cdot \tilde{\rho}_{\mu\nu} + \text{H.c.}, \quad (19)$$

with $\nabla_\mu \boldsymbol{\pi} = \frac{1}{2} \partial_\mu \boldsymbol{\pi} + f_\pi g_{A_1} \mathbf{a}_\mu + O(\pi^2)$ and $\tilde{\rho}_{\mu\nu} = \boldsymbol{\rho}_{\mu\nu} + O(\pi)$. The vector current V_μ and the axial-vector current A_μ corresponding to the effective Lagrangian of Ref. 25 are

$$\mathcal{J}^V_\mu = \frac{m_\rho^2}{g_\rho} \boldsymbol{\rho}_\mu, \quad (20)$$

$$\mathcal{J}^A_\mu = g_{A_1} \frac{m_\rho^2}{g_\rho^2} \mathbf{a}_\mu - f_\pi \partial_\mu \boldsymbol{\pi}. \quad (21)$$

The numerical values of various parameters (coupling constants and so on) to be used in the present calculation are listed in Appendix A.

The MEC contributions due to π or ρ exchange that are expected from the effective Lagrangian of the hard-pion approach are depicted in Fig. 2 (for the axial-vector current A_λ) and in Fig. 3 (for the vector current V_λ). The explicit expressions for the vertices appearing in these diagrams acting on the nuclear configuration space are obtained in the standard manner.[26] Since the effective Hamiltonian in IA, H_{eff} of Eq. (7), was obtained by retaining the terms up to $O(1/m_N)$ and since the MEC contributions are of the order of $1/m_N$ compared to the main IA terms, we consider only leading-order MEC terms in the nonrelativistic reduction of the two-body contributions. The results are summarized in Appendix B. The contributions of these MEC diagrams can be taken into account effectively by replacing the various terms in H_{eff} [Eq. (7)] in the following manner:

$$\sum_i F_A \boldsymbol{\sigma}^{(i)} \tau_-^{(i)} \rightarrow \sum_i F_A \boldsymbol{\sigma}^{(i)} \tau_-^{(i)} + \sum_{i<j} \mathbf{A}^{(2)}(i,j), \quad (22)$$

$$\sum_i F_P \boldsymbol{\sigma}_l \cdot \hat{\boldsymbol{\nu}} \boldsymbol{\sigma}^{(i)} \cdot \hat{\boldsymbol{\nu}} \tau_-^{(i)} \rightarrow \boldsymbol{\sigma}_l \cdot \hat{\boldsymbol{\nu}} \left[\sum_i F_P \boldsymbol{\sigma}^{(i)} \cdot \hat{\boldsymbol{\nu}} \tau_-^{(i)} + \sum_{i<j} P^{(2)}(i,j) \right], \quad (23)$$

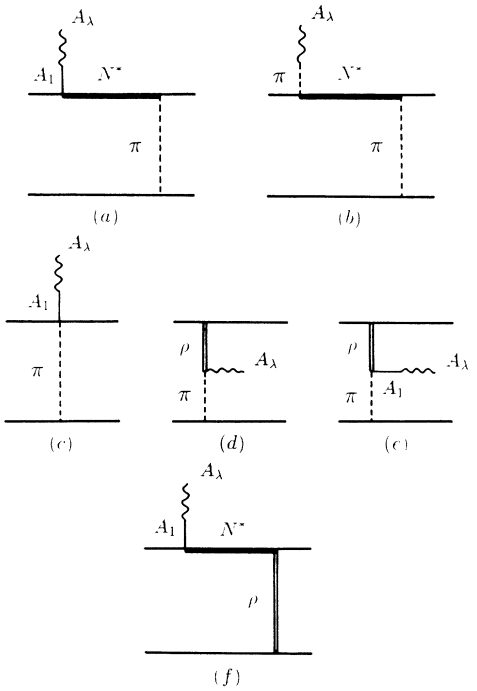

FIG. 2. Processes contributing to axial-vector exchange current in the hard-pion approach (Ref. 21). A_λ stands for the axial-vector current, while A_1 stands for the A_1 meson; the other symbols will be self-explanatory.

$$\sum_i \frac{f_V}{m_N}\boldsymbol{\sigma}_l\cdot\hat{\mathbf{v}}\boldsymbol{\sigma}_l\cdot\mathbf{P}^{(i)}\tau_-^{(i)} \rightarrow \boldsymbol{\sigma}_l\cdot\hat{\mathbf{v}}\boldsymbol{\sigma}_l\cdot\left[\sum_i \frac{f_V}{m_N}\mathbf{P}^{(i)}\tau_-^{(i)}+\sum_{i<j}\mathbf{v}^{(2)}(i,j)\right], \quad (24)$$

$$\sum_i \frac{f_A}{m_N}\boldsymbol{\sigma}_l\cdot\hat{\mathbf{v}}\boldsymbol{\sigma}^{(i)}\cdot\mathbf{P}^{(i)}\tau_-^{(i)} \rightarrow \boldsymbol{\sigma}_l\cdot\hat{\mathbf{v}}\left[\sum_i \frac{f_A}{m_N}\boldsymbol{\sigma}^{(i)}\cdot\mathbf{P}^{(i)}\tau_-^{(i)}+\sum_{i<j}a^{(2)}(i,j)\right]. \quad (25)$$

The change in Eq. (22) is due to the space component of diagrams (a), (c), (d), (e), and (f) in Fig. 2, while that in Eq. (23) is due to diagram (b) of Fig. 2. The diagrams in Fig. 3 give rise to $\mathbf{v}^{(2)}(i,j)$ in Eq. (24). Finally, the change in Eq. (25) comes from the time component of diagrams (c), (d), and (e) in Fig. 2, and $a^{(2)}(i,j)$ represents the Kubodera-Delorme-Rho (KDR) exchange current[27] in the context of the hard-pion approach. Its importance to the μd-capture neutron spectrum has been emphasized in Ref. 28.

In evaluating the nuclear matrix element of two-body operators, the short-range behavior of the two-body operators is of importance. We therefore take account of the finite size of the nucleon by attaching to each meson-baryon vertex a form factor $K_B(q^2)$ of the form

$$K_B(q^2)=\frac{\Lambda_B^2-m_B^2}{\Lambda_B^2+q^2}. \quad (26)$$

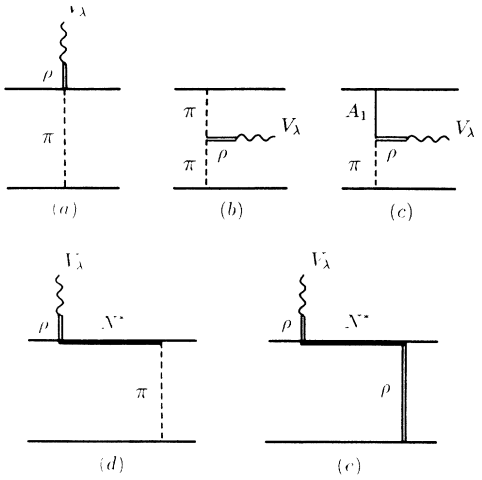

FIG. 3. Processes contributing to vector exchange current in the hard-pion approach (Ref. 21). V_λ stands for the vector current.

In this expression m_B ($B=\pi$, ρ, or A_1) is the meson mass, and Λ_B is a cutoff parameter, which is taken to be the same for the NNB and N^*NB vertices. Specifically, we use[29] $\Lambda_\pi=1.25$ GeV, $\Lambda_\rho=1.50$ GeV, and $\Lambda_{A_1}=1.85$ GeV. The introduction of the form factor $K_B(q^2)$ leads to a modification of the radial dependence of the two-body operator. The details of this modification are given in Appendix D.

For the nucleon-nucleon interaction that determines the wave functions of the initial deuteron and the final n-n scattering state, we use here three different potentials: the Reid soft-core (RSC) potential, the Reid hard-core (RHC) potential,[30] and the Paris potential.[31]

One problem here is that, if we use the phenomenological nuclear forces, the current conservation is not satisfied for the vector current. A way out is to invoke the Siegert theorem[32–34] to place a constraint on the longitudinal part of the vector current. In fact, with the extended Siegert theorem,[33] which was fully developed for photonuclear processes, one can in principle construct multipole operators for the general vector current including meson-exchange effects in such a manner that the current conservation be respected. However, in the present case where the axial current gives a dominant contribution and which involves rather high momentum transfers, the effect of incorporating the Siegert theorem is expected to be much less important than in the photonuclear reactions. We therefore use here a simplified method in which the one-body current is modified so that the current conservation is guaranteed. As will be discussed later, this simple treatment seems sufficiently accurate for our purposes.

The current conservation implies

$$\int e^{-i\mathbf{v}\cdot\mathbf{x}}\boldsymbol{\nabla}\cdot\mathbf{J}^V d^3x = -i\int e^{-i\mathbf{v}\cdot\mathbf{x}}[H,\rho]d^3x, \quad (27)$$

which can be easily rewritten as

$$\hat{\nu}\cdot\mathbf{J}^V=-\frac{E_f-E_i}{E_\nu}\rho \ . \tag{28}$$

The decomposition of the vector current J^V into one- and two-body parts, $\mathbf{J}^V=\mathbf{J}_1^V+\mathbf{J}_2^V$, leads to

$$\hat{\nu}\cdot\mathbf{J}^V=\hat{\nu}\cdot\mathbf{J}_1^V+\hat{\nu}\cdot\mathbf{J}_2^V=-\frac{E_f-E_i}{E_\nu}\rho \ . \tag{29}$$

For the one-body part $\mathbf{J}_1^V$ given by

$$\mathbf{J}_1^V=\frac{1}{2m_N}(2\mathbf{p}_i-\boldsymbol{\nu})+\frac{i}{2m_N}\boldsymbol{\nu}\times\boldsymbol{\sigma} \ , \tag{30}$$

we should have

$$\hat{\nu}\cdot\mathbf{J}_1^V=\frac{1}{m_N}(\hat{\nu}\cdot\mathbf{p}_i)-\frac{E_\nu}{2m_N} \ . \tag{31}$$

It is not a trivial task to determine an explicit form of $\mathbf{J}_2^V$ that satisfies Eq. (29). We therefore assume that by replacing the $\mathbf{J}_1^V$ term appearing in the impulse approximation expression with $-[(E_f-E_i)/E_\nu]\rho$, one can effectively take into account the contribution of the $\mathbf{J}_2^V$ term. This amounts to making, in Eq. (12), the following replacement:

$$\mathcal{M}_1\equiv F_V M_1-\frac{f_V}{m_N}(\hat{\nu}\cdot\mathbf{M}_3)$$
$$\rightarrow\frac{m_\mu}{E_\nu}f_V M_1 \ . \tag{32}$$

It is to be noted here that only spin-nonflip two-body effects can be taken into account by this procedure. Thus, in the context of μd capture, one expects that the $\mathbf{J}_2^V$ effects for the final ${}^3P_J, {}^3F_J, \ldots$ are approximately included, but that the $M1$ transitions leading to, e.g., the final ${}^1S_0$ state must be treated separately. In the present paper, the spin-nonflip vector-current transition amplitudes are obtained with prescription of Eq. (32) based on the Siegert theorem, whereas for the spin-flip vector-current transition amplitudes we evaluate explicitly the contributions of the diagrams in Fig. 3 by using the effective two-body operators derived in Appendix B.

The capture rate from the μ-d hyperfine doublet state is expressed as

$$\lambda_d=G_F^2\cos^2\theta_C\frac{1}{2\pi^2}\int dE_n\, p m_N E_\nu^2\, y_r\cdot|T_{fi}|^2 \ , \tag{33}$$

with

$$m_\mu-\varepsilon-2E_n-E_\nu-\frac{E_\nu^2}{4m_N}=0 \ ,$$

where $\mathbf{p}=(\mathbf{p}_1-\mathbf{p}_2)/2$, $E_n=\mathbf{p}^2/(2m_N)$, and $\varepsilon=2m_N-m_d$; the factor

$$y_r\equiv\frac{1}{\sqrt{1+(m_\mu-\varepsilon-2E_n)/m_N}} \ , \tag{34}$$

represents recoil correction for the center-of-mass motion of the final n-n system. $|T_{fi}|^2$ is the square of the transition matrix element for the hyperfine doublet capture integrated over the directions of $\mathbf{p}$ and $\boldsymbol{\nu}$. In the present work we do *not* introduce the "one-point" approximation for the muon wave function, $f(\mathbf{x})$ in Eq. (7), but retain the radial dependence of the muon wave function calculated for the point nuclear charge. The general expression for $|T_{fi}|^2$ is quite involved and therefore relegated to Appendix C. For the sake of comparison with the previous work,[1] it may be useful to give the expression for $|T_{fi}|^2$ for a simplified case in which the d-state component in the deuteron is taken into account only for the s-wave final n-n scattering state, and the nuclear interaction is considered only for the s-wave n-n state, all other higher-l states treated as free waves. For this simplified case, $|T_{fi}|^2$ can be written as

$$\begin{aligned}|T_{fi}|^2=&12[F_A H-\tfrac{1}{3}F_P(H+\sqrt{2}J)]^2-8(F_A-\tfrac{1}{3}F_P)f_A\frac{1}{m_N}HK\\
&+\sum_{L=\text{even},L\neq 0}^{4}(2L+1)\left[12(F_A-\tfrac{1}{3}F_P)^2H_L^2-8(F_A-\tfrac{1}{3}F_P)f_A\frac{1}{m_N}H_L K_L\right]\\
&+16\sum_{L=\text{odd}}^{5}(2L+1)\left[(\tfrac{1}{4}F_V'^2+F_A^2+\tfrac{1}{6}F_P^2-\tfrac{2}{3}F_P F_A-F_V' F_A+\tfrac{1}{3}F_P F_V')H_L^2-\tfrac{1}{3}(2F_A-F_P-F_V')f_A\frac{1}{m_N}H_L K_L\right]\\
&-8[F_A H-\tfrac{1}{3}F_P(H+\sqrt{2}J)]\left[3D_0+\frac{m_\mu\nu}{2m_N}\frac{f_P}{f_A}(D_0'+\sqrt{2}D_2')+\frac{\nu}{m_N}D_3\right]\\
&+\tfrac{8}{3}[F_A(H-2\sqrt{2}J)+F_P(H+\sqrt{2}J)]D_1 \ ,\end{aligned} \tag{35}$$

where $F_V'=(m_\mu/E_\nu)f_V$, and the radial integrals for the IA contributions are defined by

$$H=\int_0^\infty dr\frac{F_0(pr)}{p}j_0\left[\frac{\nu r}{2}\right]u(r)f\left[\frac{r}{2}\right] \ , \tag{36a}$$

$$J=\int_0^\infty dr\frac{F_0(pr)}{p}j_2\left[\frac{\nu r}{2}\right]w(r)f\left[\frac{r}{2}\right] \ , \tag{32b}$$

$$K=-\int_0^\infty r\,dr\frac{F_0(pr)}{p}j_1\left[\frac{vr}{2}\right]\frac{d}{dr}\left[\frac{u(r)}{r}\right]f\left[\frac{r}{2}\right], \tag{36c}$$

$$H_L=\int_0^\infty r\,dr\,j_L(pr)j_L\left[\frac{vr}{2}\right]u(r)f\left[\frac{r}{2}\right], \tag{36d}$$

$$K_L=\int_0^\infty r^2\,dr\,j_L(pr)\left[\frac{L}{2L+1}j_{L-1}\left[\frac{vr}{2}\right]-\frac{L+1}{2L+1}j_{L+1}\left[\frac{vr}{2}\right]\right]\frac{d}{dr}\left[\frac{u(r)}{r}\right]f\left[\frac{r}{2}\right]. \tag{36e}$$

In the above, $f(r)$ is the radial function of the muon $1s$ orbit; we use here the Bohr orbit for the point nuclear charge. The functions $u(r)$ and $w(r)$ are the deuteron s- and d-wave radial functions, respectively, and $F_0(pr)$ is the s-wave radial function for the final n-n relative motion. The terms involving D_0, D_0', D_2', D_1, and D_3 in Eq. (35) represent exchange-current contributions [D_0 arises from $A^{(2)}(i,j)$, D_0' and D_2' from $P^{(2)}(i,j)$, D_1 from $a^{(2)}(i,j)$, and D_3 from $\mathbf{v}^{(2)}(i,j)$], and the explicit expressions of D_0, D_0', D_2', D_1, and D_3 are given in Appendix D. If we drop from the above equations the terms of $O(p/m_N)$, i.e., K and K_L, the resulting expressions are identical with those given by DRR except for the following points: (1) the exchange currents here are derived from the hard-pion approach, (2) the variation of the muon wave function over the nuclear volume is taken into account here, and (3) the present treatment includes the MEC effects for the vector current, which were dropped in DRR.

III. NUMERICAL RESULTS

Table I gives the numerical results calculated with the standard values [Eq. (14)] of the nucleon weak-interaction form factors. It is to be observed that the results for the three different potentials have only minor differences, and therefore we can discuss them collectively. We see from this table that, in the IA without the exchange current, $\lambda_d^{\text{theor}}=364$–$369\ \text{s}^{-1}$ and that the contribution of the terms of $O(p/m_N)$ is about 2 orders of magnitude smaller than the leading terms of $O(1)$; this checks with the results reported by Pascual *et al.*[3] The inclusion of the meson-exchange current substantially increases the capture rate, leading to $\lambda_d^{\text{theor}}=397$–$400\ \text{s}^{-1}$. Thus λ_d^{theor} obtained with the standard framework of the IA plus exchange-current effects is in good agreement with $\lambda_d^{\text{expt}}=409\pm40\ \text{s}^{-1}$ of Ref. 13, but disagrees with $\lambda_d^{\text{expt}}=470\pm29\ \text{s}^{-1}$ reported in Ref. 12.

The present calculation includes the MEC effects for both the vector and axial-vector currents, whereas the previous work[1,2] took into account only the axial-vector current MEC. Table I indicates that 70% of the MEC contribution is due to the axial-vector current, while the newly calculated vector current MEC constitutes the remaining 30%. Of the axial-vector current MEC, the predominant part comes from the space component, the time component (corresponding to the KDR current[27]) adding to λ_d^{theor} only $\sim0.5\ \text{s}^{-1}$. This is in conformity with the general consideration of KDR.[27] We remark that the MEC effects are sensitive to two-nucleon short-range correlation; the MEC contributions given in Table I would become larger by a factor of ~1.4 if the short-range correlation were ignored.

We have considered here not only the pion-exchange but also the ρ-exchange diagrams (see Figs. 2 and 3). The contributions of the ρ-exchange processes are as follows. (We take as an example the case of the RSC potential.) Of the axial-vector current MEC contribution, $22.0\ \text{s}^{-1}$, the ρ-exhange part is $-8.5\ \text{s}^{-1}$. Of the $M1$-type vector current contribution, $7.8\ \text{s}^{-1}$, the ρ-exchange part gives $-1.0\ \text{s}^{-1}$. Thus the ρ-exchange current plays a significant role in the axial-vector current MEC and $M1$-type vector current MEC, which have been calculated through the explicit evaluation of the Feynman diagrams in Figs. 2 and 3.

As explained earlier, the $E1$-type vector current contribution is estimated by invoking the Siegert theorem instead of using the Feynman diagrams. Table I indicates that the effect of incorporating the Siegert theorem through the prescription of Eq. (32) is to increase λ_d^{theor}

TABLE I. Total capture rate λ_d^{theor} in units of s^{-1} calculated with the standard values of the nucleon weak-interaction form factors given in Eq. (14). Three different nuclear potentials are used: the Reid soft-core potential (RSC), the Reid hard-core potential (RHC), and the Paris potential. For each case are given λ_d^{theor} and its decomposition into various individual contributions.

	RSC	RHC	Paris
Final state $L=0$	232.0	230.9	233.5
Final state $L=1$	118.6	118.9	120.6
Final state $L=2$	6.9	6.9	7.0
Final state $L=3$	3.0	3.0	3.1
$1\le L\le5$	128.8	129.1	131.0
$O(1)$	360.8	360.0	364.5
$O\left[\frac{p}{m_\nu}\right]$	4.4	4.4	4.5
$\text{IA}=O(1)+O\left[\frac{p}{m_\nu}\right]$	365.2	364.4	369.0
MEC (axial)	22.0	22.7	19.9
KDR	0.5	0.4	0.5
MEC (vector $\{M_1\}$)	7.8	7.6	7.8
Siegert theorem	2.3	2.4	2.4
MEC (total)	32.6	33.1	30.6
$\lambda_d^{\text{theor}}=\text{IA}+\text{MEC}$ (total)	397.8	397.5	399.6

by $\sim 2\ s^{-1}$. An independent calculation by the Osaka group[28] based on the extended Siegert theorem shows a similar tendency.

We have taken into account in this work the radial dependence of the muon wave function without invoking the one-point approximation. This improvement has been found to decrease λ_d^{theor} by $6\ s^{-1}$.

We now discuss the effects of deviations of the nucleon weak-interaction form factors from the standard values. The form factors f_V, f_W, and f_A are already well determined empirically so that the freedom of variation, if any, exists only with f_S, f_T, and f_P. The conserved vector-current (CVC) hypothesis dictates that $f_S=0$, but no such restriction exists for the second-class axial-vector current form factor f_T. There have been a great many experimental works[35] to obtain information on f_T, and a chi-squares fitting[36] to the totality of the existing nuclear β-decay data yielded $|f_T(0)| \leq |f_W(0)|/2.5$ at the 90% confidence level. We will examine the maximum possible change in λ_d^{theor} when $|f_T(0)|$ is allowed to vary within this empirical upper limit. Since our purpose here is to obtain an estimate of the maximum possible change, we may ignore the q^2 dependence of $f_T(q^2)$. As for the choice of pseudoscalar form factor, the influence of variation in f_P was discussed in Ref. 1. We examine here the joint effects of deviations of f_T and f_P from their standard values. To this end, we will allow f_P to deviate from the standard value by the amount compatible with the precision with which the Goldberger-Treiman relation has been tested.[37] To be specific, by introducing $\beta \equiv f_P(0)/[f_P(0)]_{\text{standard}}$ with $[f_P(0)]_{\text{standard}} = 2m_N f_A(0)/m_\pi^2$ given by Eq. (14d), we consider the three cases $\beta=1$ and 1 ± 0.1. Here, again, we only deal with possible changes in the overall strength of f_P, keeping the q^2 dependence of $f_P(q^2)$ fixed as given by Eq. (14d).

The results for nonstandard values of f_T and f_P are given in Tables II–IV. We can see from these tables that, even if we allow for the maximum possible change of the single-nucleon form factors, it is impossible to obtain λ_d^{theor} as large as $\lambda_d^{\text{expt}}=470\pm 29\ s^{-1}$ reported in Ref. 12. The maximum value within the present framework (corresponding to the choice $\beta=0.9$, $f_T=-f_W/2.5$, and the Paris potential) is $\lambda_d^{\text{theor}}=422\ s^{-1}$, which is significantly smaller than the lower end of the experimental value given in Ref. 12.

Ahrens *et al.*[38] recently derived a stringent upper limit to the second-class current strength from an analysis of high-energy ν_μ-p scattering data. The target of this experiment consists of complex nuclei as well as protons, but it is argued that the analysis is free from nuclear-medium effects once the quasifree kinematical region is selected. In our opinion, however, this argument may require a closer examination. As exemplified by the $e+d \rightarrow e+n+p$ reaction wherein substantial exchange-current effects are observed even in the kinematical region involving large momentum transfers,[7] there may be nuclear-medium effects that were not reckoned with in the analysis of Ref. 38. Until this point is clarified, we should probably take the conclusion of Ref. 38 with some reservation. This is why we have used here the upper limit to f_T determined in Ref. 36, although this may turn out to be too generous an allowance for f_T, once the above-mentioned ambiguity is removed. Anyway, the use of the upper limit $|f_T| \leq |f_W|/2.5$ will serve the purpose of demonstrating that even the most generous allowance for f_T cannot reproduce λ_d^{expt} of Ref. 12.

We explain here some technical details concerning the truncation scheme used in the present calculation. The number of partial waves in the final n-n system that can be included in actual numerical calculations is limited for practical reasons. We show in Table V how many partial waves in the final state have been taken into account, depending on the importance of transition operators in question. Table V also indicates which cases contain both the s- and d-state components in the initial deuteron

TABLE II. Capture rate λ_d in units of s^{-1} calculated with the Reid soft-core potential. The breakdown of λ_d into the impulse approximation term and the exchange-current contribution is also shown; the former is further decomposed into the contributions of $O(1)$ and $O(p/M)$. Case (a) corresponds to the standard choice of f_T, i.e., $f_T=0$, as expressed in Eq. (14f), whereas cases (b) and (c) correspond, respectively, to $f_T=f_W/2.5$ and $-f_W/2.5$, the maximum allowed magnitude described in the text. For each of these cases, the row with $\beta=1$ corresponds to the use of the standard value of f_P as given in Eq. (14d), whereas the rows with $\beta=1\pm 0.1$ represent possible deviations from the standard value. The standard results corresponding to the choice of the form factors given in Eq. (14) are underlined.

f_T	β	$O(1)$	$O(p/m_N)$	Exchange	Total
	0.9	368.3	4.5	33.0	405.8
(a) 0	1.0	360.8	4.4	32.6	397.8
	1.1	353.3	4.4	32.3	390.0
	0.9	355.4	4.4	32.4	392.2
(b) $f_W/2.5$	1.0	348.0	4.4	32.0	384.4
	1.1	340.7	4.3	31.6	376.6
	0.9	381.4	4.5	33.6	419.5
(c) $-f_W/2.5$	1.0	373.7	4.5	33.2	411.4
	1.1	366.1	4.5	32.9	403.5

TABLE III. Capture rate λ_d in units of s^{-1} calculated with the Reid hard-core potential. For further explanations, see the caption of Table II.

f_I	β	$O(1)$	$O(p/m_\nu)$	Exchange	Total
	0.9	367.4	4.4	33.5	405.3
(a) 0	1.0	360.0	4.4	33.1	397.5
	1.1	352.5	4.3	32.8	389.6
	0.9	354.6	4.3	32.9	391.8
(b) $f_W/2.5$	1.0	347.2	4.3	32.5	384.0
	1.1	339.9	4.3	32.2	376.4
	0.9	380.5	4.4	34.2	419.1
(c) $-f_W/2.5$	1.0	372.8	4.4	33.8	411.0
	1.1	365.2	4.4	33.4	403.0

wave function and which cases include only the s-state component. As can be seen from Table V, the present calculation takes into account considerably more components of the two-nucleon wave functions than in the work of Sotona and Truhlik.[3] The main purpose of this generalization is to recheck the validity of the truncation scheme DRR used on the base of the work of Sotona and Truhlik.[3] To this end, we have carried out a calculation in which only those components appearing in Eq. (35) are retained (Table VI). By comparing the results of the two calculations, we reconfirmed that the truncation scheme used in Ref. 1 changes λ_d by less than 0.5 s^{-1} and thus has a sufficient accuracy for the present purpose.

In comparing the present results with those in the literature, we need to recall that the previous works[1,2] used $f_A(0)=-1.25$, a value that was standard at the time of those calculations. Furthermore, the "one-point" approximation for the muon wave function was employed, and $f(r)$ was fixed at its value at $r=0$. So, for the sake of comparison, we have repeated our calculation using the old value $f_A(0)=-1.25$ and the one-point approximation. The results are summarized in Table VII, from which one can see that there are significant discrepancies between the previous and present calculations; the old value of λ_d due to the leading-order IA terms is larger by as much as ~ 20 s^{-1}. We could not trace the origin of this difference.[42] The only comment we can make here is that, if we ignore the recoil correction in our treatment by setting $y_r=1$, the results (given as TKK$^{(\#)}$ in Table VII) agree very well with the previous ones. [Note that the difference in modeling the exchange current explains the difference between the MEC contribution in DRR (Ref. 1) and that in Ivanov and Truhlik[2] (IT) and TKK.]

We summarize this section as follows. We have corroborated the conclusion that it is difficult to explain $\lambda_d^{\rm expt}=470\pm29$ s^{-1} reported in Ref. 12 within the standard framework of the IA supplemented by meson-exchange effects; on the other hand, the present results are in good agreement with $\lambda_d^{\rm expt}=409\pm40$ s^{-1} obtained in Ref. 13. In this situation,[46] we tentatively take the view that the agreement between $\lambda_d^{\rm expt}$ of Ref. 13 and $\lambda_d^{\rm theor}$ supports the present theoretical framework more strongly than the disagreement between $\lambda_d^{\rm expt}$ of Ref. 12 and $\lambda_d^{\rm theor}$ disproves it. To the extent that this view is tenable, the calculational method used here is reliable up to the experimental accuracy achieved in Ref. 13, i.e., at the 10% level, for the intermediate-energy weak process involving the $A=2$ nuclear system. Needless to say, we should await the clarification of the experimental situa-

TABLE IV. Capture rate λ_d in units of s^{-1} calculated with the Paris potential. For further explanations, see the caption of Table II.

f_I	β	$O(1)$	$O(p/m_\nu)$	Exchange	Total
	0.9	372.1	4.5	31.0	407.6
(a) 0	1.0	364.5	4.5	30.6	399.6
	1.1	356.9	4.4	30.3	391.6
	0.9	359.1	4.5	30.4	394.0
(b) $f_W/2.5$	1.0	351.6	4.4	30.0	386.0
	1.1	344.2	4.4	29.7	378.3
	0.9	385.4	4.6	31.5	421.5
(c) $-f_W/2.5$	1.0	377.6	4.5	31.2	413.3
	1.1	369.9	4.5	30.9	405.3

TABLE V. Chart to show which components in the initial and final two-nucleon wave functions have been included in obtaining the results shown in Tables I–IV. The circles and double circles indicate components that have been included. For the double-circled entries the nuclear interaction in the final n-n system have been taken into account, while the single-circled entries have been treated as free waves.

Operators		Component in deuteron	Partial waves in final n-n system $L=0$	$L=1$	$L=2$	$L=3$	$L=4$	$L=5$
IA	$O(1)$	s	⊙	⊙	⊙	○	○	○
		d	⊙	⊙	⊙			
	$O\left[\frac{p}{m_\Lambda}\right]$	s	⊙	○	○	○	○	
Exch.	A_1N^*	s	⊙	⊙	⊙			
		d	⊙	⊙	⊙			
	others	s	⊙					
		d	⊙					

tion before making any final conclusion, but we consider it reasonable to take this view as a working hypothesis when estimating the neutrino-deuteron reaction cross sections in the next section. We should add that for lower-energy neutrinos ($E_\nu \leq 20$ MeV), where the well-established IA term dominates, the calculational method used here is reliable with a few percent precision.

IV. CROSS SECTIONS FOR ν-d And $\bar{\nu}$-d REACTIONS

A. Calculational method

As mentioned in Sec. I, reasonably reliable estimates of the cross sections for $\nu(\bar{\nu})$-d reactions are in great demand for extracting useful astrophysical information from data that would become available from the planned heavy-water Čerenkov counter at Sudbury.[10] One of the great advantages of the heavy-water Čerenkov counter is that it can detect both the neutral-current and charged-current reactions, and record them separately. As was emphasized in Ref. 39, the detection of neutral-current reactions is crucially important for testing the Mikheyev-Smirnov-Wolfenstein (MSW) mechanism[40] as a possible solution for the solar neutrino problem.[9] Furthermore, the detection of both the neutral-current and charged-current reactions enables us to determine the neutrino mass difference by measuring arrival time delays of supernova neutrinos.[18]

We evaluate here the cross sections for ν-d and $\bar{\nu}$-d reactions for medium energies ($E_\nu \leq 170$ MeV) in the framework of the impulse approximation (IA) supplemented by the exchange current. The validity of this approach in this kinematical region has been tested in the electromagnetic process[7] and in the μ-d capture treated in the preceding sections. As stated at the end of Sec. III, the experimental situation with the μd capture rate is yet to be clarified, but we are here tentatively assuming that the good agreement between $\lambda_d^{\rm expt}$ of Ref. 13 and $\lambda_d^{\rm theor}$ supports the calculational method used here. With this working hypothesis accepted, the present calculation is expected to be reliable at the $\sim 10\%$ level for $E_\nu \leq 170$ MeV.[41] On the other hand, for lower incident energies, $E_\nu \leq 20$ MeV, this method is known to be reliable up to the level of a few percent.

TABLE VI. Comparison of the "truncated" calculation with the "full" calculation. For each of the three nuclear potentials, the row labeled (a) gives $\lambda_d^{\rm theor}$ and its breakdown into the various individual contributions calculated with the use of the simplified formula for $|T_{fi}|^2$ [Eq. (35)]. The row labeled (b) gives the results obtained with the full expression for $|T_{fi}|^2$ given in Eq. (C9).

Potential		$O(1)$	$O(p/m_\Lambda)$	Exchange	Total
RSC	(a)	361.0	4.4	31.9	397.3
	(b)	360.8	4.4	32.6	397.8
RHC	(a)	360.4	4.4	32.5	397.3
	(b)	360.0	4.4	33.1	397.5
Paris	(a)	364.8	4.5	30.0	399.3
	(b)	364.5	4.5	30.6	399.6

TABLE VII. Comparison with the previous works. DRR: Dautry *et al.* (Ref. 1); IT: Ivanov and Truhlik (Ref. 2); TKK: present work. The row labeled TKK$^{(\pi)}$ represents the case in which the recoil correction is artificially neglected, i.e., $y_r = 1$. In the row labeled IT, the entry 38* was deduced by rescaling the corresponding entry in Ref. 2 by the ratio $f_{\pi NN^*}(\Delta\text{-width})/f_{\pi NN^*}(\text{quark model})$.

	IA($O(1)$)	Exch.	Total
DRR	381	24	405
IT	380	38*	418
TKK	362	35	397
TKK$^{(\pi)}$	381	37	418

Apart from the use of the hard-pion approach, the main differences between the present treatment and that of Refs. 17 and 18 are as follows: (i) The effects of finite momentum transfers are taken into account by retaining the form factor $j_l(qr)$; (ii) for the relative motion of the outgoing two-nucleon system, we include partial waves up to $l \leq 5$, whereas only the $l=0$ state was considered in Refs. 17 and 18; and (iii) the MEC are considered in a more systematic way. That is, both the vector current and axial-vector current MEC contributions are evaluated here using the hard-pion approach[2,21] (with the supplementary use of the Siegert theorem for the spin-nonflip vector current transitions). In Ref. 18, mainly because of the neglect of partial waves higher than the s state, the theoretical cross sections were assigned relative errors of $\sim 50\%$ for incident energy as low as $E_\nu \sim 50$ MeV. The improved calculation described here can significantly reduce theoretical uncertainties.

We are concerned with the calculation of cross sections for the charged-current reactions:

$$\nu_e + d \rightarrow e^- + p + p \ , \tag{37a}$$

$$\bar{\nu}_e + d \rightarrow e^+ + n + n \ , \tag{37b}$$

and cross sections for the neutral-current reactions:

$$\nu + d \rightarrow \nu' + n + p \ , \tag{38a}$$

$$\bar{\nu} + d \rightarrow \bar{\nu}' + n + p \ . \tag{38b}$$

Since the treatment of the charged-current reaction is exactly the same as that of the μ capture apart from trivial Hermitian conjugation necessary for dealing with the inverse process, we can immediately write down the cross section σ_{cc}:

$$\sigma_{cc} \equiv \int dE_n \, d\Omega_e \frac{1}{\pi^3} \frac{e_0 e p m_N}{1+(e_0-\nu_0 z)/2m_N} \times G_F^2 \cos^2\theta_C F(Z_f, e_0) |T|^2 \ , \tag{39}$$

where ν_0 and $\boldsymbol{\nu}$ are the energy and momentum of the neutrino, e_0 and $\mathbf{e}$ are the energy and momentum of the electron or positron, $e=|\mathbf{e}|$, $z=\hat{\boldsymbol{\nu}}\cdot\hat{\mathbf{e}}$, $\mathbf{p}=(\mathbf{p}_1-\mathbf{p}_2)/2$, $E_n=\mathbf{p}^2/(2m_N)$, and $F(Z_f,e_0)$ is the Fermi factor. The transition matrix element squared $|T|^2$ is given with good accuracy by

$$\begin{aligned}
|T|^2 = f_A^2 \Bigg\{ & [1-\tfrac{1}{3}(\hat{\boldsymbol{\nu}}\cdot\hat{\mathbf{e}})](H^2+J^2) + [(\hat{\boldsymbol{\nu}}\cdot\hat{\mathbf{q}})(\hat{\mathbf{e}}\cdot\hat{\mathbf{q}}) - \tfrac{1}{3}(\hat{\boldsymbol{\nu}}\cdot\hat{\mathbf{e}})]J(2\sqrt{2}H+J) \\
& \mp \frac{4}{3f_A}(f_V - 2m_N f_W)\frac{1}{2m_N}[(\hat{\boldsymbol{\nu}}\cdot\mathbf{q})-(\hat{\mathbf{e}}\cdot\mathbf{q})]\left[H-\frac{1}{\sqrt{2}}J\right]^2 - \frac{1}{3m_N}[(\hat{\mathbf{e}}\cdot\mathbf{q})+(\hat{\boldsymbol{\nu}}\cdot\mathbf{q})](H+\sqrt{2}J)^2 \Bigg] \\
& + \sum_{L=\text{even}} (2L+1)H_L^2 f_A^2 \left[[1-\tfrac{1}{3}(\hat{\boldsymbol{\nu}}\cdot\hat{\mathbf{e}})] \mp \frac{4}{3f_A}(f_V - 2m_N f_W)\frac{1}{2m_N}[(\hat{\boldsymbol{\nu}}\cdot\mathbf{q})-(\hat{e}\cdot\mathbf{q})] - \frac{1}{3m_N}[(\hat{\mathbf{e}}\cdot\mathbf{q})+(\hat{\boldsymbol{\nu}}\cdot\mathbf{q})] \right] \\
& + \sum_{L=\text{odd}} (2L+1)H_L^2 \Bigg[[1+(\hat{\boldsymbol{\nu}}\cdot\hat{\mathbf{e}})]\frac{q_\lambda^2}{\mathbf{q}^2} f_V^2 + 2[1-\tfrac{1}{3}(\hat{\boldsymbol{\nu}}\cdot\hat{\mathbf{e}})]f_A^2 \mp \tfrac{8}{3} f_A (f_V - 2m_N f_W)\frac{1}{2m_N}[(\hat{\boldsymbol{\nu}}\cdot\mathbf{q})-(\hat{\mathbf{e}}\cdot\mathbf{q})] \\
& \qquad - (f_V^2 + \tfrac{2}{3}f_A^2)\frac{1}{m_N}[(\hat{\mathbf{e}}\cdot\mathbf{q})+(\hat{\boldsymbol{\nu}}\cdot\mathbf{q})] \Bigg] \\
& - 2f_A \{ [1-\tfrac{1}{3}(\hat{\boldsymbol{\nu}}\cdot\hat{\mathbf{e}})](HD_0 + JD_2) + [(\hat{\boldsymbol{\nu}}\cdot\hat{\mathbf{q}})(\hat{\mathbf{e}}\cdot\hat{\mathbf{q}}) - \tfrac{1}{3}(\hat{\boldsymbol{\nu}}\cdot\hat{\mathbf{e}})][\sqrt{2}JD_0 + (\sqrt{2}H+J)D_2] \} \\
& \pm \tfrac{2}{3}(f_V - 2m_N f_W)\frac{1}{m_N}[(\hat{\boldsymbol{\nu}}\cdot\mathbf{q})-(\hat{\mathbf{e}}\cdot\mathbf{q})]\left[H-\frac{1}{\sqrt{2}}J\right]\left[D_0 - \frac{1}{\sqrt{2}}D_2\right] \\
& + \frac{f_A}{3m_N}[(\hat{\boldsymbol{\nu}}\cdot\mathbf{q})+(\hat{\mathbf{e}}\cdot\mathbf{q})](H+\sqrt{2}J)(D_0+\sqrt{2}D_2) \mp \tfrac{2}{3} f_A \frac{1}{m_N}[(\hat{\boldsymbol{\nu}}\cdot\mathbf{q})-(\hat{\mathbf{e}}\cdot\mathbf{q})]\left[H-\frac{1}{\sqrt{2}}J\right]D_3 \ ,
\end{aligned} \tag{40}$$

with

$$H = \int_0^\infty dr \frac{F_0(pr)}{p} j_0\left(\frac{qr}{2}\right) u(r) \ , \tag{41a}$$

$$J = \int_0^\infty dr \frac{F_0(pr)}{p} j_2\left(\frac{qr}{2}\right) w(r) \ , \tag{41b}$$

$$H_L = \int_0^\infty r\, dr\, j_L(pr) j_L\left(\frac{qr}{2}\right) u(r) \ . \tag{41c}$$

Here the upper (lower) sign corresponds to the neutrino (antineutrino) reaction, and $q_\lambda = \nu_\lambda - e_\lambda$; the electron mass has been neglected. The radial integrals D_0, D_2, and D_3 for the exchange-current contribution have already appeared in connection with Eq. (35), and their explicit expressions are given in Appendix D. [In the actual calculation, we drop the contribution of the KDR current[27] and that of diagram (c) in Fig. 3, since their roles in the μd capture have been found to be small. We also remark that the contribution of diagram (b) of Fig. 2,

being proportional to the lepton mass, can be ignored in the present context.] In writing down Eq. (40), we have taken into account the final-state nucleon-nucleon interaction only for the s wave, since our experience with the μ-d capture indicates that it is a good approximation to ignore the nuclear interaction for higher partial waves. For the p-p final state, however, it is understood that $j_L(pr)$ appearing in the definition of H_L [Eq. (41c)] should be replaced by the regular Coulomb radial function.

For the neutral-current process, we start with the effective Hamiltonian

$$H_{\rm eff}^{\rm nc}=\frac{G_F}{\sqrt{2}}J_\mu^{(0)}L_\mu \ . \tag{42}$$

The lepton current L_μ is written as $L_\mu=-i\bar{u}_\nu\gamma_\mu(1+\gamma_5)u_\nu$ for the reaction (38a) and $L_\mu=-i\bar{v}_\nu\gamma_\mu(1+\gamma_5)v_\nu$ for the reaction (38b). The hadronic neutral current $J_\mu^{(0)}$ in the standard (Weinberg-Salam-Glashow-Iliopoulos-Maiani) model is given by

$$J_\mu^{(0)}=V_\mu^3+A_\mu^3-2\sin^2\theta_W(V_\mu^S+V_\mu^3) \ . \tag{43}$$

Here V_μ^S is the isoscalar vector current, V_μ^i ($i=1,2,3$) the isovector vector current, and A_μ^i ($i=1,2,3$) the isovector axial-vector current; θ_W ($\sin^2\theta_W=0.23$) is the Weinberg angle. Obviously, $J_\mu^{(0)}$ has both isoscalar and isovector parts:

$$J_\mu^{(0)}=J_\mu^{T=0}+J_\mu^{T=1} \ , \tag{44}$$

with

$$J_\mu^{T=0}=-2\sin^2\theta_W V_\mu^S \ ,$$
$$J_\mu^{T=1}=(1-2\sin^2\theta_W)V_\mu^3+A_\mu^3 \ . \tag{45}$$

In the neutral-current reactions Eqs. (38a) and (38b), the final n-p state can have both $T=0$ and 1. This implies that the isoscalar and isovector currents can interfere in general. However, for angle-averaged, spin-independent observables, there is no interference between the isoscalar and isovector contributions for the following reason. The channel spin of the final n-p system can be used as one of the quantum numbers to specify final states. This implies that the contribution of spin-triplet and spin-singlet final states can be added incoherently with no interference between them. Meanwhile, averaging over the orientation of the n-p relative motion eliminates interference between partial waves of different parities. Since the spin and parity of a two-nucleon state uniquely determine its isospin, we can conclude that there is no interference between the isotriplet and isosinglet final states. This situation renders the role of isoscalar contributions practically negligible. On the other hand, the dominant isovector neutral current is simply related to the charged current by a rotation in isospin space (apart from the difference in the coupling constants). Thus we can work with the effective Hamiltonian

$$H_{\rm eff}^{\rm nc}=H_{\rm eff}^{\rm IA}+H_{\rm eff}^{\rm MEC} \ , \tag{46}$$

where

$$H_{\rm eff}^{\rm IA}=-\frac{G_F}{\sqrt{2}}\sum_{i=1,2}\left[\left[if_V'+\frac{i}{2m_N}f_A\boldsymbol{\sigma}^{(i)}\cdot\mathbf{q}\right]L_4^*(\mathbf{r}_i)+\left[f_A\boldsymbol{\sigma}^{(i)}+\frac{i}{2m_N}(f_V'-2m_Nf_W')\boldsymbol{\sigma}^{(i)}\times\mathbf{q}+\frac{1}{2m_N}f_V'\mathbf{q}\right]\cdot\mathbf{L}^*(\mathbf{r}_i)\right]\frac{\tau_3^{(i)}}{2} \ , \tag{47}$$

with

$$f_V'=(1-2\sin^2\theta_W)f_V, \quad f_W'=(1-2\sin^2\theta_W)f_W \ .$$

Following the above discussion, we only have to consider the MEC for the dominant isovector current. Then the MEC contribution of relevance can be written as

$$H_{\rm eff}^{\rm MEC}=\frac{G_F}{\sqrt{2}}\mathbf{J}_{\rm MEC}\cdot\mathbf{L}^*(\mathbf{r}_i) \ , \tag{48}$$

where $\mathbf{J}_{\rm MEC}$ is obtained from $\mathbf{A}^{(2)}(i,j)$ and $\mathbf{v}^{(2)}(i,j)$ [see Eqs. (22)–(25) and Appendix B] by changing $\pm$ into 3. We note here again that we need not consider the exchange current coming from diagram (b) of Fig. 2, whose contribution is proportional to the lepton mass. Furthermore, we ignore the KDR current and the contribution of diagram (c) of Fig. 3 since their roles in the μd capture rate were very minor.

The cross section $\sigma_{\rm nc}$ for the neutral-current reaction is given by

$$\sigma_{\rm nc}\equiv\int dE_n\,d\Omega_e\frac{1}{2\pi^3}\frac{e_0epm_N}{1+(e_0-\nu_0z)/2m_N}G_F^2|T|^2 \ , \tag{49}$$

where e_0 and $\mathbf{e}$ are the energy and momentum of the final neutrino, $e=|\mathbf{e}|$, and $z=\hat{\nu}\cdot\hat{\mathbf{e}}$. For the contribution of the isovector part of the hadronic current, the transition matrix element squared $|T|^2$ is given, with the same approximation as for Eq. (40), by

$$
\begin{aligned}
|T|^2 = f_A^2 \Bigg\{ & [1-\tfrac{1}{3}(\hat{\nu}\cdot\hat{e})](H^2+J^2)+[(\hat{\nu}\cdot\hat{q})(\hat{e}\cdot\hat{q})-\tfrac{1}{3}(\hat{\nu}\cdot\hat{e})]J(2\sqrt{2}H+J) \\
& \mp \frac{4}{3f_A}(f_V'-2m_N f_W')\frac{1}{2m_N}[(\hat{\nu}\cdot\mathbf{q})-(\hat{e}\cdot\mathbf{q})]\left[H-\frac{1}{\sqrt{2}}J\right]^2-\frac{1}{3m_N}[(\hat{e}\cdot\mathbf{q})+(\hat{\nu}\cdot\mathbf{q})](H+\sqrt{2}J)^2\Bigg] \\
& + \sum_{L=\text{even}}(2L+1)H_L^2 f_A^2\left[[1-\tfrac{1}{3}(\hat{\nu}\cdot\hat{e})]\mp\frac{4}{3f_A}(f_V'-2m_N f_W')\frac{1}{2m_N}[(\hat{\nu}\cdot\mathbf{q})-(\hat{e}\cdot\mathbf{q})]-\frac{1}{3m_N}[(\hat{e}\cdot\mathbf{q})+(\hat{\nu}\cdot\mathbf{q})]\right] \\
& + \sum_{L=\text{odd}}(2L+1)H_L^2\Bigg[[1+(\hat{\nu}\cdot\hat{e})]\frac{q_\lambda^2}{\mathbf{q}^2}f_V'^2+2[1-\tfrac{1}{3}(\hat{\nu}\cdot\hat{e})]f_A^2\mp\tfrac{8}{3}f_A(f_V'-2m_N f_W')\frac{1}{2m_N}[(\hat{\nu}\cdot\mathbf{q})-(\hat{e}\cdot\mathbf{q})] \\
& \qquad -(f_V'^2+\tfrac{2}{3}f_A^2)\frac{1}{m_N}[(\hat{e}\cdot\mathbf{q})+(\hat{\nu}\cdot\mathbf{q})]\Bigg] \\
& -2f_A\{[1-\tfrac{1}{3}(\hat{\nu}\cdot\hat{e})](HD_0+JD_2)+[(\hat{\nu}\cdot\hat{q})(\hat{e}\cdot\hat{q})-\tfrac{1}{3}(\hat{\nu}\cdot\hat{e})][\sqrt{2}JD_0+(\sqrt{2}H+J)D_2]\} \\
& \pm\tfrac{2}{3}(f_V-2m_N f_W)\frac{1}{m_N}[(\hat{\nu}\cdot\mathbf{q})-(\hat{e}\cdot\mathbf{q})]\left[H-\frac{1}{\sqrt{2}}J\right]\left[D_0-\frac{1}{\sqrt{2}}D_2\right] \\
& +\frac{f_A}{3m_N}[(\hat{\nu}\cdot\mathbf{q})+(\hat{e}\cdot\mathbf{q})](H+\sqrt{2}J)(D_0+\sqrt{2}D_2)\mp\tfrac{2}{3}f_A\frac{1}{m_N}[(\hat{\nu}\cdot\mathbf{q})-(\hat{e}\cdot\mathbf{q})]\left[H-\frac{1}{\sqrt{2}}J\right]D_3 ,
\end{aligned}
\tag{50}
$$

where the upper (lower) sign corresponds to the neutrino (antineutrino) reaction. If we ignore in Eq. (50) the terms that involve the n-p partial waves other than the s wave, the corresponding cross section should agree with the expression given by Eqs. (17) and (18) in Ref. 18. From this comparison, we have found that Eq. (18) of Ref. 18 involves an error; the factor $\pm\frac{1}{3}$ should read $\pm\frac{2}{3}$. This completes the explanation of our calculational method, and numerical results will be presented in Sec. IV B.

B. Numerical results

In calculating the charged-current reaction cross sections σ_{cc} [Eq. (39)] and the neutral-current reaction cross section σ_{nc} [Eq. (49)], we use the standard values of the nucleon weak-interaction form factors listed in Eq. (14) and the Reid soft-core potential. The results of the calculation of the μ-d capture rate indicate that using the other potentials (the Reid hard-core and Paris potentials) will lead to practically the same results. The estimates of the cross sections are shown in Table VIII and in Figs. 4 and 5. As remarked earlier, these cross sections are considered to be reliable at the $\sim 10\%$ level for incident energies $E_\nu \leq 170$ MeV; for lower-energy neutrinos, $E_\nu \leq 20$ MeV, where the well-established IA terms give overwhelmingly dominant contributions, the reliability is expected to be better than a few percent.

Regarding the neutral-current reaction cross sections, there are two comments to be made here. The first is concerned with charge-dependent effects in the two-nucleon system. As is well known, the scattering length a_{np} for the spin-singlet n-p system is different from the scattering length a_{nn} for the n-n system; $a_{np}=-23.7$ fm, while $a_{nn}=-18.7\pm0.6$ fm.[47] Since the original Reid potential[30] does not take account of the charge dependence, we need to modify the Reid potential for the n-p channel slightly so that $a_{np}=-23.7$ fm is reproduced. To achieve this, we have changed, as in Ref. 18, the strength of the nonpion part of the Reid potential. The results given in Table VIII and Fig. 5 have been obtained after applying

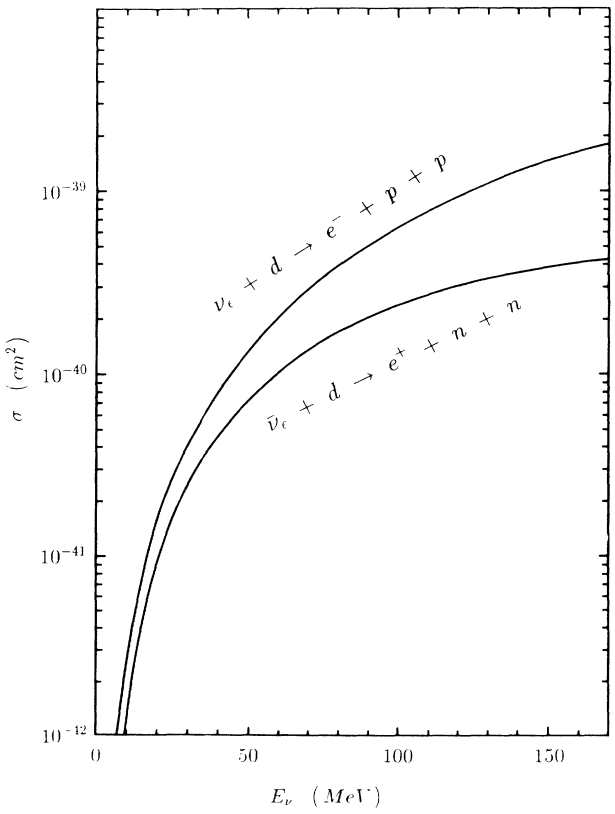

FIG. 4. Cross sections for charged-current processes.

TABLE VIII. Total cross sections for neutrino reactions on deuteron calculated as functions of the incident neutrino energy E_ν. The Reid soft-core potential was used.

E_ν (MeV)	$d(\nu,\nu')np$ $\times 10^{-42}$ cm^2	$d(\bar{\nu},\bar{\nu}')np$ $\times 10^{-42}$ cm^2	$d(\nu,e^-)pp$ $\times 10^{-42}$ cm^2	$d(\bar{\nu},e^+)nn$ $\times 10^{-42}$ cm^2
4	0.0307	0.0302	0.158	
6	0.201	0.196	0.624	0.116
8	0.554	0.534	1.46	0.515
10	1.10	1.05	2.71	1.23
12	1.86	1.75	4.37	2.27
14	2.82	2.62	6.48	3.63
16	3.99	3.67	9.05	5.30
18	5.38	4.90	12.1	7.28
20	6.99	6.29	15.6	9.55
25	12.0	10.5	26.6	16.5
30	18.4	15.7	40.9	25.0
35	26.3	21.8	58.7	35.1
40	35.7	28.8	80.1	46.5
45	46.6	36.6	105	59.2
50	59.1	45.2	134	72.9
60	88.4	64.3	204	103
70	124	85.7	289	136
80	165	109	390	170
90	211	133	506	205
100	262	158	635	239
110	317	184	777	272
120	375	209	930	303
130	437	235	1090	333
140	502	259	1260	360
150	568	284	1440	384
160	637	307	1630	406
170	706	330	1820	425

this modification. The effect of the charge dependence is expected to be more pronounced in the low-energy region, wherein the role of the nuclear final-state interaction is more significant. Our explicit calculation indicates that the introduction of the charge-dependent effect enhances $\sigma(\nu d \to \nu' np)$ and $\sigma(\bar{\nu} d \to \bar{\nu}' np)$ by 11% for $E_\nu = 4$ MeV, 3.7% for $E_\nu = 10$ MeV, 2.1% for $E_\nu = 20$ MeV, and 0.8% for $E_\nu = 50$ MeV. We have checked that this feature is practically independent of choices between (slightly) different nuclear potentials, so long as these potentials reproduce $a_{np} = -23.7$ fm.

The second comment is concerned with the isoscalar neutral current, $J_\mu^{T=0} = -2\sin^2\theta_W V_\mu^S$. As discussed earlier in the text, the absence of interference between the isovector and isoscalar contributions to the total cross section leads us to expect that the role of the isoscalar current will be minor. To ascertain this expectation, we have calculated explicitly the contribution of the isoscalar current in IA, and have found that it increases $\sigma_{\rm nc}$ only by a few percent even at $E_\nu \sim 150$ MeV. (For low incident energies, the isoscalar transition operator reduces to the unit operator and hence cannot give rise to any nuclear transitions.) Since this is within uncertainties of the present calculational method itself, we can ignore the isoscalar neutral current altogether.

Since solar neutrinos relevant to the deuterium detector are the ^{8}B-decay neutrinos and the *hep* neutrinos,[9] we

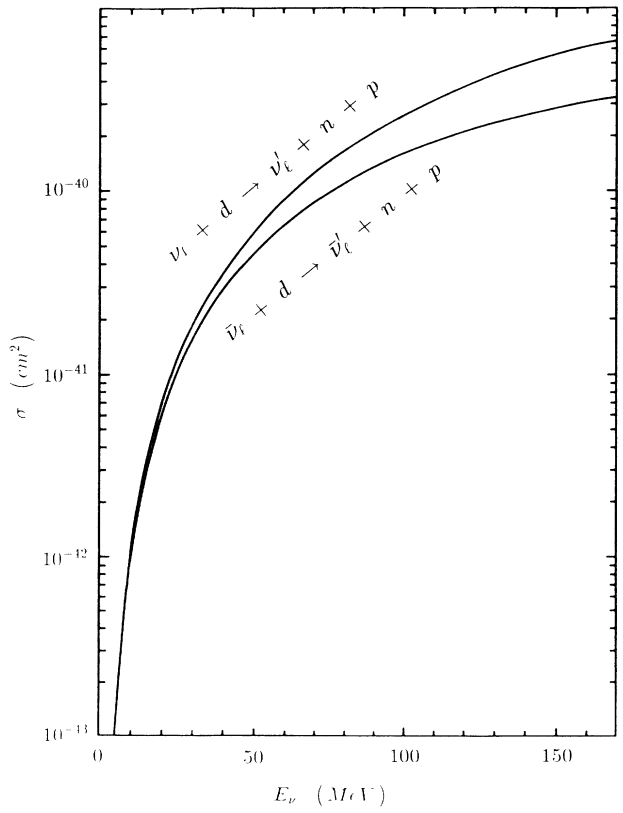

FIG. 5. Cross sections for neutral-current processes.

have calculated the neutrino-deuteron cross sections averaged over the spectra for the ^{8}B decay[9,43] and *hep* neutrinos.[9] The results for the charged-current reactions are

$$\langle \sigma_{cc}(^8\mathrm{B}) \rangle = 1.22 \times 10^{-42} \text{ cm}^2 , \quad (51a)$$

$$\langle \sigma_{cc}(hep) \rangle = 3.14 \times 10^{-42} \text{ cm}^2 , \quad (51b)$$

while those for the neutral-current reactions are

$$\langle \sigma_{nc}(^8\mathrm{B}) \rangle = 4.72 \times 10^{-43} \text{ cm}^2 , \quad (52a)$$

$$\langle \sigma_{nc}(hep) \rangle = 1.32 \times 10^{-42} \text{ cm}^2 . \quad (52b)$$

We note that $\langle \sigma_{nc}(^8\mathrm{B}) \rangle$ obtained here is $\sim 15\%$ larger than the corresponding value in Ref. 18. [The inclusion of the charge-dependent effect increases $\langle \sigma_{nc}(^8\mathrm{B}) \rangle$ by $\sim 5\%$ both in the present work and in Ref. 18.] With the use of these new estimates together with the ^{8}B-neutrino and *hep*-neutrino fluxes obtained from the standard solar model,[9] we can calculate the event rates of deuterium disintegration in the one-kiloton D_2O Sudbury Neutrino Observatory. The results are (the 100% detection efficiency assumed)

$$\text{charged-current events} \simeq \begin{cases} 1.35(1 \pm 0.38) \times 10^4 \text{ yr}^{-1} \text{ kt}^{-1}, & \text{for } ^8\text{B neutrino} , \\ 4.54(1 \pm 0.38) \times 10^1 \text{ yr}^{-1} \text{ kt}^{-1}, & \text{for } hep \text{ neutrino} , \end{cases} \quad (53)$$

$$\text{neutral-current events} \simeq \begin{cases} 5.21(1 \pm 0.38) \times 10^3 \text{ yr}^{-1} \text{ kt}^{-1}, & \text{for } ^8\text{B neutrino} , \\ 1.91(1 \pm 0.38) \times 10^1 \text{ yr}^{-1} \text{ kt}^{-1}, & \text{for } hep \text{ neutrino} . \end{cases} \quad (54)$$

These event rates are expected to contain 38% errors due to uncertainties in the neutrino flux[9] calculated in the standard solar model. (The uncertainties in the estimated cross sections themselves are negligible in this context.)

The neutrinos produced in a supernova explosion approximately obey the Fermi-Dirac (FD) or Maxwell-Boltzmann (MB) spectrum.[44] We therefore give in Table IX (Table X) the cross sections averaged over the FD (MB) spectrum. Convenient fitting formulas for these results are as follows.

Charged current reactions:

$$\langle \sigma_{pp}(\mathrm{FD}) \rangle = (3.35 T_\nu^{2.31} - 3.70) \times 10^{-43} \text{ cm}^2 , \quad (55a)$$

$$\langle \sigma_{nn}(\mathrm{FD}) \rangle = (3.05 T_\nu^{2.08} - 7.82) \times 10^{-43} \text{ cm}^2 , \quad (55b)$$

$$\langle \sigma_{pp}(\mathrm{MB}) \rangle = (3.06 T_\nu^{2.31} - 3.42) \times 10^{-43} \text{ cm}^2 , \quad (56a)$$

$$\langle \sigma_{nn}(\mathrm{MB}) \rangle = (2.75 T_\nu^{2.09} - 7.09) \times 10^{-43} \text{ cm}^2 . \quad (56b)$$

Neutral-current reactions:

$$\langle \sigma_{\nu}(\mathrm{FD}) \rangle = (1.63 T_\nu^{2.26} - 2.78) \times 10^{-43} \text{ cm}^2 , \quad (57a)$$

$$\langle \sigma_{\bar{\nu}}(\mathrm{FD}) \rangle = (2.03 T_\nu^{2.05} - 3.76) \times 10^{-43} \text{ cm}^2 , \quad (57b)$$

$$\langle \sigma_{\nu}(\mathrm{MB}) \rangle = (1.50 T_\nu^{2.26} - 2.61) \times 10^{-43} \text{ cm}^2 , \quad (58a)$$

$$\langle \sigma_{\bar{\nu}}(\mathrm{MB}) \rangle = (1.87 T_\nu^{2.05} - 3.58) \times 10^{-43} \text{ cm}^2 . \quad (58b)$$

Given a supernova explosion model that predicts the temperature of neutrinos and antineutrinos of different flavors as well as their fluences, one can easily calculate, as Bahcall *et al.*[18] did, the event rates expected at the Sudbury Neutrino Observatory. It is generally expected[44] that the temperature $T(\nu_e)$ of the electron neutrinos is typically 4–5 MeV, whereas the temperature of muonic and tau neutrinos is somewhat higher, 8–10 MeV. For the sake of definiteness, let us take $T(\nu_e) = T(\bar{\nu}_e) = 5$ MeV and $T(\nu_\mu) = T(\bar{\nu}_\mu) = T(\nu_\tau) = T(\bar{\nu}_\tau) = 10$ MeV. Furthermore, let us use the following typical neutrino fluences:[18]

TABLE IX. Total cross sections for neutrino reactions on deuteron averaged over the Fermi-Dirac spectrum with temperature T_ν. The Reid soft-core potential was used.

T_ν (MeV)	$d(\nu,\nu')np$ $\times 10^{-42}$ cm^2	$d(\bar{\nu},\bar{\nu}')np$ $\times 10^{-42}$ cm^2	$d(\nu,e^-)pp$ $\times 10^{-42}$ cm^2	$d(\bar{\nu},e^+)nn$ $\times 10^{-42}$ cm^2
2	0.524	0.493	1.31	0.582
3	1.62	1.49	3.79	2.05
4	3.41	3.03	7.74	4.47
5	5.90	5.11	13.3	7.80
6	9.12	7.69	20.5	12.0
7	13.1	10.7	29.5	16.9
8	17.8	14.2	40.3	22.5
9	23.2	18.1	52.9	28.8
10	29.4	22.4	67.2	35.6

TABLE X. Total cross sections for neutrino reactions on deuteron averaged over the Maxwell-Boltzmann spectrum with temperature T_ν. The Reid soft-core potential was used.

T_ν (MeV)	$d(\nu,\nu')np$ $\times 10^{-42}$ cm^2	$d(\bar{\nu},\bar{\nu}')np$ $\times 10^{-42}$ cm^2	$d(\nu,e^-)pp$ $\times 10^{-42}$ cm^2	$d(\bar{\nu},e^+)nn$ $\times 10^{-42}$ cm^2
2	0.477	0.450	1.20	0.528
3	1.49	1.36	3.47	1.87
4	3.13	2.78	7.12	4.09
5	5.42	4.70	12.2	7.16
6	8.39	7.09	18.9	11.0
7	12.1	9.92	27.2	15.6
8	16.4	13.2	37.1	20.8
9	21.4	16.8	48.8	26.6
10	27.1	20.7	62.0	32.9

$$\phi(\nu_e)=2.4\times 10^{11}\ \text{cm}^{-2}\left[\frac{8\ \text{kpc}}{\text{distance}}\right]^2,$$

$$\phi(\nu_\mu)=\phi(\bar{\nu}_\mu)=\phi(\nu_\tau)=\phi(\bar{\nu}_\tau)=1.7\times 10^{11}\ \text{cm}^{-2}\left[\frac{8\ \text{kpc}}{\text{distance}}\right]^2,$$

$$\phi(\bar{\nu}_e)\sim 0.7\phi(\nu_e)\ .$$

For these values, we expect

$$\text{total charged-current events}\simeq\begin{cases}2.71\times 10^2\left[\dfrac{8\ \text{kpc}}{\text{distance}}\right]^2, & \text{for FD}, \quad (59a)\\ 2.48\times 10^2\left[\dfrac{8\ \text{kpc}}{\text{distance}}\right]^2, & \text{for MB}, \quad (59b)\end{cases}$$

$$\text{total neutral-current events}\simeq\begin{cases}1.20\times 10^3\left[\dfrac{8\ \text{kpc}}{\text{distance}}\right]^2, & \text{for FD}, \quad (60a)\\ 1.10\times 10^3\left[\dfrac{8\ \text{kpc}}{\text{distance}}\right]^2, & \text{for MB}. \quad (60b)\end{cases}$$

Finally, for the sake of completeness, we give in Table XI the cross sections averaged over the spectra of the neutrinos emitted in the muon decay. As is well known, the electron-neutrino spectrum is given as $dN(E_\nu)(\text{electron})=(192/m_\mu^4)(m_\mu/2-E_\nu)E_\nu^2 dE_\nu$, while the muon-neutrino spectrum as $dN(E_\nu)(\text{muon})=(64/m_\mu^4)(\frac{3}{4}m_\mu-E_\nu)E_\nu^2\,dE_\nu$.

It will be useful to summarize here the main points of improvements we have made over the treatment of Bahcall, Kubodera, and Nozawa[18] (BKN). (1) We have included the partial waves for the final N-N relative motion up to $l=5$, whereas BKN considered only the $l=0$ wave. (2) We have taken account of the effects of finite momentum transfers by retaining the factor $j_l(qr)$ coming from the retardation expansion, while BKN, in treating the $l=0$ wave, used an approximation $j_0(qr)\simeq 1$. (3) BKN

TABLE XI. Total cross sections for neutrino reactions on deuteron averaged over the μ-decay neutrino spectrum. The Reid soft-core potential was used.

Neutrino	$d(\nu,\nu')np$ $\times 10^{-41}$ cm^2	$d(\bar{\nu},\bar{\nu}')np$ $\times 10^{-41}$ cm^2	$d(\nu,e^-)pp$ $\times 10^{-41}$ cm^2	$d(\bar{\nu},e^+)nn$ $\times 10^{-41}$ cm^2
$\langle\nu_e\rangle(\langle\bar{\nu}_e\rangle)$	2.42	1.97	5.43	3.16
$\langle\nu_\mu\rangle(\langle\bar{\nu}_\mu\rangle)$	3.35	2.66		

calculated the meson-exchange effects only for the axial-vector current, but we have evaluated the meson-exchange contributions to the vector current as well; the spin-nonflip contribution has been estimated by the use of the Siegert theorem, while the spin-flip contribution by the explicit calculation of the Feynman diagrams in Fig. 3. The influences of these improvements become progressively more important as the incident neutrino energy increases.[45]

V. DISCUSSION AND SUMMARY

We have made a detailed calculation of λ_d, the rate of muon capture by the deuteron from the doublet hyperfine state, in the standard framework of the impulse approximation (IA) supplemented by exchange-current effects. For taking into account the exchange current, we have used the hard-pion approach,[2,21] which incorporates current algebra, PCAC, and the vector-meson dominance, and which provides a natural framework for treating the soft-pion limit and processes involving finite momentum transfers on the same footing. The effect of the vector-current conservation has been included by invoking the Siegert theorem. Furthermore, the radial dependence of the muon wave function has been retained without invoking the "one-point" approximation. For the standard choice of the nucleon weak-interaction form factors, we have obtained $\lambda_d^{\text{theor}}=397$–$400\ \text{s}^{-1}$, the small variation coming from the use of three different nuclear forces (the Reid soft-core, Reid hard-core, and Paris potentials). The change in λ_d^{theor} caused by the variation of the nucleon weak-interaction form factors within the known limits turns out to be small. Thus it is extremely difficult to explain $\lambda_d^{\text{expt}}=470\pm29\ \text{s}^{-1}$ reported in Ref. 12 within the framework of the IA supplemented with the exchange-current contributions.[46] On the other hand, the λ_d^{theor} obtained in the present calculation agrees well with $\lambda_d^{\text{expt}}=409\pm40\ \text{s}^{-1}$ given in Ref. 13.

In the same theoretical framework as used for the μ-d capture, we have calculated the cross sections for the neutrino-deuteron reactions, which are of great current interest in connection with the Sudbury project[10] to build a large heavy-water Čerenkov counter. For both the charged-current and neutral-current reactions, we have evaluated the cross sections up to $E_\nu=170$ MeV. To the extent that the agreement between λ_d^{expt} of Ref. 13 and λ_d^{theor} can be taken as evidence for the validity of the present calculational method, the cross sections obtained here are expected to be reliable at the $\sim10\%$ level for intermediate-energy neutrinos ($E_\nu\leq170$ MeV). For lower incident energies ($E_\nu\leq20$ MeV), the present results are reliable at the 2–3 % level. The estimates of the cross sections given here are expected to be of value in studying astrophysical neutrinos with the use of the planned heavy-water Čerenkov counter.[10] Obviously, it is very important to settle down the controversy on the experimental values of λ_d, and we hope that this will be done soon.

ACKNOWLEDGMENTS

We are deeply obliged to Professor H. Ohtsubo and Dr. S. Nozawa for many useful discussions, and to Dr. K. Tamura for his generous help with the use of a computer code for solving the two-nucleon problem with the Paris potential. One of the authors (K.K.) wishes to thank Professor E. M. Henley for the information of Ref. 45, received prior to publication. He is also thankful to Professor E. Truhlik for bringing his attention to the work cited in Ref. 46.

APPENDIX A

The values of the parameters used in the present work are as follows. Masses: $m_p=938.272$ MeV, $m_n=939.573$ MeV, $m_d=1875.628$ MeV, $m_{N^*}=1232$ MeV, $m_\pi=138.13$ MeV, $m_\rho=776$ MeV, and $m_{A_1}=\sqrt{2}m_\rho$; the pion decay constant: $f_\pi=93$ MeV. The coupling constants:

$$g_{A_1}=g_\rho,\quad \frac{g_\rho^2}{4\pi}=2.77,\quad \frac{f_{\pi NN}^2}{4\pi}=0.08\ . \tag{A1}$$

For the πNN^* coupling constant, we use the value determined from the Δ-decay width:

$$\frac{f_{\pi NN^*}^2}{4\pi}=0.35\ . \tag{A2}$$

Note that this value is larger than the quark-model value by 50%. As for the tensor coupling constant κ_V, we use

$$\kappa_V=3.7\ , \tag{A3}$$

for the weak interaction vertex, and

$$\kappa_V=6.6\ , \tag{A4}$$

for the strong interaction vertex. Furthermore, to determine the ρNN^* coupling constant, we make use of the relation $(g_\rho G_1/m_N)^2=(f_{\rho NN^*}/m_\rho)^2$ together with the quark-model value

$$\frac{f_{\rho NN^*}^2}{4\pi}=\frac{72}{25}\left[\frac{g_\rho}{2}\right]^2\left[\frac{m_\rho}{2m_N}\right]^2(1+\kappa_V)^2\frac{1}{4\pi}\ , \tag{A5}$$

and obtain

$$G_1^2=\tfrac{9}{50}(1+\kappa_V)^2\ . \tag{A6}$$

APPENDIX B

We give here explicit expressions for the two-body operators corresponding to the exchange current processes given in Figs. 2 and 3.

(i) The two-body operator $\mathbf{A}^{(2)}(i,j)$ appearing in Eq. (22) describes the exchange current for the space component of the axial-vector current due to diagrams (a), (c), (d), (e), and (f) in Fig. 2, and can be correspondingly decomposed as

$$\mathbf{A}^{(2)}(i,j)=\mathbf{J}^A(\mathrm{a})+\mathbf{J}^A(\mathrm{c})+\mathbf{J}^A(\mathrm{d})+\mathbf{J}^A(\mathrm{e})+\mathbf{J}^A(\mathrm{f}) . \tag{B1}$$

Although the explicit expressions were given by Ivanov and Truhlik,[21] we reproduce them here for the sake of completeness. The generic form $\mathbf{J}^A$ for $\mathbf{J}^A$(a) and $\mathbf{J}^A$(c) is written as

$$\mathbf{J}^A=(\tau_1\times\tau_2)^-\{C_1[\tfrac{1}{3}(\sigma_1\times\sigma_2)f_1-\tfrac{1}{2}\mathbf{T}_{[\sigma_1\times\sigma_2]}f_2]+C_2 i[\tfrac{1}{3}(\sigma_1-\sigma_2)f_3+\mathbf{T}_{[\sigma_1-\sigma_2]}f_4]\}+(\tau_1-\tau_2)^-C_3[\tfrac{1}{3}(\sigma_1-\sigma_2)f_5+\mathbf{T}_{[\sigma_1-\sigma_2]}f_6] , \tag{B2}$$

where

$$\mathbf{T}_{[A]}\equiv\hat{\mathbf{r}}(\hat{\mathbf{r}}\cdot\mathbf{A})-\tfrac{1}{3}\mathbf{A} , \tag{B3}$$

and f_i's are radial functions to be described below, $\mathbf{r}=\mathbf{r}_1-\mathbf{r}_2$, $\hat{\mathbf{r}}=\mathbf{r}/|\mathbf{r}|$, and C_i's numerical constants. The individual expressions for these two operators are as follows.

$\mathbf{J}^A$(a): N^* excitation term with pion exchange (A_1 current),

$$C_1=-\frac{2}{9}\frac{m_\pi f_A}{m_N^*-m_N}\frac{f_{\pi NN^*}}{4\pi},\quad C_2=0,\quad C_3=-C_1 , \tag{B4}$$

$$f_1=f_5=Y_0(x_\pi),\quad f_2=f_6=Y_2(x_\pi),\quad f_3=f_4=0 , \tag{B5}$$

where

$$x_\pi=m_\pi r ,$$
$$Y_0(x_\pi)=\frac{e^{-x_\pi}}{x_\pi} , \tag{B6}$$
$$Y_2(x_\pi)=\left[1+\frac{3}{x_\pi}+\frac{3}{x_\pi^2}\right]Y_0(x_\pi) .$$

$\mathbf{J}^A$(c): Contact term,

$$C_1=-\frac{m_\pi^3}{4\pi}\frac{f_A}{8m_N f_\pi^2}(1+\kappa_V) ,$$
$$C_2=-\frac{m_\pi^3}{4\pi}\frac{f_A}{8m_N f_\pi^2}\frac{1}{2} , \tag{B7}$$
$$C_3=0 ,$$
$$f_1=f_3=Y_0(x_\pi),\quad f_2=f_4=Y_2(x_\pi),\quad f_5=f_5=0 . \tag{B8}$$

The generic form $\mathbf{J}^A$ for $\mathbf{J}^A$(d) and $\mathbf{J}^A$(e) is written as

$$\mathbf{J}^A=(\tau_1\times\tau_2)^-\{C_1[\tfrac{1}{3}(\sigma_1\times\sigma_2)f_1-\tfrac{1}{2}\mathbf{T}_{[\sigma_1\times\sigma_2]}f_2]+C_2 i[\tfrac{1}{3}\sigma_2 f_3+\mathbf{T}_{[\sigma_2]}f_4]\}+(1\leftrightarrow 2) . \tag{B9}$$

The individual expressions for these two operators are as follows.

$\mathbf{J}^A$(d): ρ-π current contribution,

$$C_1=-\frac{1}{8\pi}\frac{f_A m_\rho^2}{8m_N f_\pi^2}(1+\kappa_V),\quad C_2=\frac{1}{8\pi}\frac{f_A m_\rho^2}{8m_N f_\pi^2} , \tag{B10a}$$

$$f_1=f_3=\int_0^1 d\alpha\, e^{-ar+i\alpha\nu\cdot\tau}g_1(r,\alpha) ,$$
$$f_2=f_4=\int_0^1 d\alpha\, e^{-ar+i\alpha\nu\cdot\tau}g_2(r,\alpha) , \tag{B10b}$$
$$g_1(r,\alpha)=a-\frac{2}{r},\quad g_2(r,\alpha)=a+\frac{1}{r} ,$$
$$a=[(1-\alpha)\alpha\nu^2+\alpha(m_\rho^2-m_\pi^2)+m_\pi^2]^{1/2} . \tag{B11}$$

$\mathbf{J}^A$(e): $A_1\rho\pi$ contribution,

$$C_1=-\frac{1}{8\pi}\frac{f_A}{8m_N f_\pi^2}(1+\kappa_V),\quad C_2=\frac{1}{8\pi}\frac{f_A}{8m_N f_\pi^2} , \tag{B12a}$$

$$f_1=f_3=\int_0^1 d\alpha\, e^{-ar+i\alpha\nu\cdot\tau}g_4(r,\alpha) ,$$
$$f_2=f_4=\int_0^1 d\alpha\, e^{-ar+i\alpha\nu\cdot\tau}g_5(r,\alpha) , \tag{B12b}$$
$$g_4(r,\alpha)=a^2\left[a-\frac{4}{r}\right] ,$$
$$g_5(r,\alpha)=a^2\left[a-\frac{1}{r}\right]-\frac{6}{r^2}\left[a+\frac{1}{r}\right] .$$

$\mathbf{J}^A$(f): N^* excitation term with ρ-meson exchange (A_1 current),

$$\mathbf{J}^A(f)=(\tau_1\times\tau_2)^-\{C_1[\tfrac{1}{3}(\sigma_1\times\sigma_2)f_1+\tfrac{1}{4}\mathbf{T}_{[\sigma_1\times\sigma_2]}f_2]+(\tau_1-\tau_2)^-C_3[\tfrac{1}{3}(\sigma_1-\sigma_2)f_5-\tfrac{1}{2}\mathbf{T}_{[\sigma_1-\sigma_2]}f_6]\} , \tag{B13}$$

$$C_1=\frac{8}{9}f_\pi\frac{f_{\pi NN^*}}{m_\pi}g_\rho\frac{G_1}{m_N}\frac{m_\rho^2}{m_A^2}\frac{m_\pi^3}{4\pi}\times g_\rho\frac{1+\kappa_V}{2m_N}\frac{1}{m_N^*-m_N} , \tag{B14a}$$
$$C_3=-C_1 ,$$
$$f_1=f_5=Y_0(x_\rho),\quad f_2=f_6=Y_2(x_\rho) , \tag{B14b}$$

with

$$x_\rho=m_\rho r .$$

(ii) The operator $P^{(2)}(i,j)$ in Eq. (23) is the exchange current for the axial-vector current due to diagram (b) of Fig. 2:

$$P^{(2)}(i,j)=\{(\tau_1\times\tau_2)^-C_1[\tfrac{1}{3}(\sigma_1\times\sigma_2)\cdot\nu f_1-\tfrac{1}{2}\mathbf{T}_{[\sigma_1\times\sigma_2]}\cdot\nu f_2]+(\tau_1-\tau_2)^-C_3[\tfrac{1}{3}(\sigma_1-\sigma_2)\cdot\nu f_5+\mathbf{T}_{[\sigma_1-\sigma_2]}\cdot\nu f_6]\}\frac{m_\mu}{\nu^2+m_\pi^2} , \tag{B15}$$

where

$$C_1=-\frac{2}{9}\frac{m_\pi f_A}{m_N^*-m_N}\frac{f_{\pi NN^*}}{4\pi},\quad C_3=-C_1\ , \tag{B16a}$$

$$f_1=f_5=Y_0(x_\pi),\quad f_2=f_6=Y_2(x_\pi),\quad f_3=f_4=0\ . \tag{B16b}$$

(iii) The operator $\mathbf{v}^{(2)}(i,j)$ in Eq. (24) represents the exchange current for the vector current and consists of five terms corresponding to diagrams (a)–(e) in Fig. 3:

$$\mathbf{v}^{(2)}(i,j)=\mathbf{J}^V(\mathrm{a})+\mathbf{J}^V(\mathrm{b})+\mathbf{J}^V(\mathrm{c})+\mathbf{J}^V(\mathrm{d})+\mathbf{J}^V(\mathrm{e})\ . \tag{B17}$$

The individual contributions are as follows.

$\mathbf{J}^V$(a): Contact term,

$$\mathbf{J}^V(\mathrm{a})=C_V^{(\mathrm{a})}\tfrac{1}{2}[(\boldsymbol{\tau}_1\times\boldsymbol{\tau}_2)^-\boldsymbol{\sigma}_1(\boldsymbol{\sigma}_2\cdot\hat{\mathbf{r}})Y_1(x_\pi)+(1\leftrightarrow2)]\ , \tag{B18a}$$

$$C_V^{(\mathrm{a})}=4\left[\frac{f_A}{2f_\pi}\right]^2\frac{m_\pi^2}{4\pi}\ . \tag{B18b}$$

$\mathbf{J}^V$(b): Mesonic current contribution,

$$\mathbf{J}^V(\mathrm{b})=-iE_\nu C_V^{(\mathrm{b})}\tfrac{1}{2}\left\{(\boldsymbol{\tau}_1\times\boldsymbol{\tau}_2)^-\int_0^1 d\alpha\left[\left[a+\frac{1}{r}\right]\hat{\mathbf{r}}(\boldsymbol{\sigma}_1\cdot\hat{\boldsymbol{\nu}})(\boldsymbol{\sigma}_2\cdot\hat{\mathbf{r}})-\frac{1}{r}(\boldsymbol{\sigma}_1\cdot\hat{\boldsymbol{\nu}})\boldsymbol{\sigma}_2\right]e^{-ar+i\alpha\nu\cdot\hat{\mathbf{r}}}+(1\leftrightarrow2)\right\}\ , \tag{B19a}$$

$$C_V^{(\mathrm{b})}=\frac{2}{3}\left[\frac{f_A}{2f_\pi}\right]^2\frac{1}{4\pi}\ . \tag{B19b}$$

$$a=[(1-\alpha)\alpha\nu^2+m_\pi^2]^{1/2}\ . \tag{B19c}$$

$\mathbf{J}^V$(c): $A_1\rho\pi$ contribution,

$$\mathbf{J}^V(\mathrm{c})=-iE_\nu C_V^{(\mathrm{c})}\frac{1}{2}\left\{(\boldsymbol{\tau}_1\times\boldsymbol{\tau}_2)^-\int_0^1 d\alpha\left[\left[a+\frac{1}{r}\right]\hat{\boldsymbol{\nu}}\times(\hat{\mathbf{r}}\times\boldsymbol{\sigma}_1)(\hat{\mathbf{r}}\cdot\boldsymbol{\sigma}_2)+\frac{1}{r}\hat{\boldsymbol{\nu}}\times(\boldsymbol{\sigma}_1\times\boldsymbol{\sigma}_2)\right]e^{-ar+i\alpha\nu\cdot\hat{\mathbf{r}}}+(1\leftrightarrow2)\right\}\ , \tag{B20a}$$

$$C_V^{(\mathrm{c})}=\frac{2}{3}\left[\frac{f_A}{2f_\pi}\right]^2\frac{1}{4\pi}\ . \tag{B20b}$$

$$a=[(1-\alpha)\alpha\nu^2+\alpha(m_{A_1}^2-m_\pi^2)+m_\pi^2]^{1/2}\ . \tag{B20c}$$

$\mathbf{J}^V$(d): N^* excitation term with pion exchange (ρ current),

$$\begin{aligned}\mathbf{J}^V(\mathrm{d})=-iE_\nu C_V^{(\mathrm{d})}\tfrac{1}{2}&[(\boldsymbol{\tau}_1-\boldsymbol{\tau}_2)^-(\{(\hat{\boldsymbol{\nu}}\times\hat{\mathbf{r}})[(\boldsymbol{\sigma}_1-\boldsymbol{\sigma}_2)\cdot\hat{\mathbf{r}}]-\tfrac{1}{3}[\hat{\boldsymbol{\nu}}\times(\boldsymbol{\sigma}_1-\boldsymbol{\sigma}_2)]\}Y_2(x_\pi)+\tfrac{1}{3}[\hat{\boldsymbol{\nu}}\times(\boldsymbol{\sigma}_1-\boldsymbol{\sigma}_2)]Y_0(x_\pi))\\&+(\boldsymbol{\tau}_1\times\boldsymbol{\tau}_2)^-\{[\hat{\boldsymbol{\nu}}\times(\hat{\mathbf{r}}\times\boldsymbol{\sigma}_1)(\boldsymbol{\sigma}_2\cdot\hat{\mathbf{r}})+\tfrac{1}{3}\hat{\boldsymbol{\nu}}\times(\boldsymbol{\sigma}_1\times\boldsymbol{\sigma}_2)]Y_2(x_\pi)-\tfrac{1}{3}[\hat{\boldsymbol{\nu}}\times(\boldsymbol{\sigma}_1\times\boldsymbol{\sigma}_2)]Y_0(x_\pi)\}+(1\leftrightarrow2)]\ ,\end{aligned} \tag{B21a}$$

$$C_V^{(\mathrm{d})}=-\frac{f_A}{2f_\pi g_\rho}\left[g_\rho\frac{G_1}{m_N}\right]\frac{f_{\pi NN^*}^2}{4\pi}\frac{8}{9}\frac{m_\pi^2}{m_N^*-m_N}\ . \tag{B21b}$$

$\mathbf{J}^V$(e): N^* excitation term with ρ-meson exchange (ρ current),

$$\begin{aligned}\mathbf{J}^V(\mathrm{e})=-iE_\nu C_V^{(\mathrm{e})}\tfrac{1}{2}&[(\boldsymbol{\tau}_1-\boldsymbol{\tau}_2)^-(\{(\hat{\boldsymbol{\nu}}\times\hat{\mathbf{r}})[(\boldsymbol{\sigma}_1-\boldsymbol{\sigma}_2)\cdot\hat{\mathbf{r}}]-\tfrac{1}{3}[\hat{\boldsymbol{\nu}}\times(\boldsymbol{\sigma}_1-\boldsymbol{\sigma}_2)]\}Y_2(x_\rho)-\tfrac{2}{3}[\hat{\boldsymbol{\nu}}\times(\boldsymbol{\sigma}_1-\boldsymbol{\sigma}_2)]Y_0(x_\rho))\\&+(\boldsymbol{\tau}_1\times\boldsymbol{\tau}_2)^-\{[\hat{\boldsymbol{\nu}}\times(\hat{\mathbf{r}}\times\boldsymbol{\sigma}_1)(\boldsymbol{\sigma}_2\cdot\hat{\mathbf{r}})+\tfrac{1}{3}\hat{\boldsymbol{\nu}}\times(\boldsymbol{\sigma}_1\times\boldsymbol{\sigma}_2)]Y_2(x_\rho)+\tfrac{2}{3}[\hat{\boldsymbol{\nu}}\times(\boldsymbol{\sigma}_1\times\boldsymbol{\sigma}_2)]Y_0(x_\rho)\}+(1\leftrightarrow2)]\ ,\end{aligned} \tag{B22a}$$

$$C_V^{(\mathrm{e})}=\frac{1}{2m_N}(1+\kappa_V)\left[g_\rho\frac{G_1}{m_N}\right]^2\frac{1}{4\pi}\frac{4}{9}\frac{m_\rho^3}{m_N^*-m_N}\ . \tag{B22b}$$

(iv) The operator $a^{(2)}(i,j)$ in Eq. (25) accounts for the exchange current for the time component of the axial-vector current and has contributions from diagrams (c), (d), and (e) of Fig. 2:

$$a^{(2)}(i,j)=J_4^A(\mathrm{c})+J_4^A(\mathrm{d})+J_4^A(\mathrm{e})\ . \tag{B23}$$

Explicit expressions for the individual terms are as follows.

J_4^A(c): Contact term,

$$J_4^A(\mathrm{c})=(\boldsymbol{\tau}_1\times\boldsymbol{\tau}_2)^-C_K^{(\mathrm{c})}i[\hat{\mathbf{r}}\cdot(\boldsymbol{\sigma}_1-\boldsymbol{\sigma}_2)]f_3\ , \tag{B24}$$

where

$$C_K^{(c)}=-\frac{m_\pi^2}{4\pi}\frac{f_A}{4f_\pi^2}\frac{1}{2}\ , \tag{B25a}$$

$$f_3=Y_1(x_\pi)\ , \tag{B25b}$$

with

$$Y_1(x_\pi)=\left[1+\frac{1}{x_\pi}\right]Y_0(x_\pi)\ . \tag{B26}$$

The contributions of diagrams (d) and (e) are both of the form

$$J_4^A=(\tau_1\times\tau_2)^-C_K i(\hat{\mathbf{r}}\cdot\boldsymbol{\sigma}_2)f_3+(1\leftrightarrow 2)\ . \tag{B27}$$

J_4^A(d): ρ-π current contribution,

$$C_K^{(d)}=\frac{m_\rho^2}{8\pi}\frac{f_A}{4f_\pi^2}\ , \tag{B28a}$$

$$f_3=\int_0^1 d\alpha\, e^{-ar+i\alpha\nu\cdot\mathbf{r}}\ . \tag{B28b}$$

J_4^A(e): $A_1\rho\pi$ contribution,

$$C_K^{(e)}=\frac{1}{8\pi}\frac{f_A}{4f_\pi^2}\ , \tag{B29a}$$

$$f_3=\int_0^1 d\alpha\, e^{-ar+i\alpha\nu\cdot\mathbf{r}}g_3(r,\alpha)\ , \tag{B29b}$$

where

$$g_3(r,\alpha)=a^2-\frac{2}{r}a-\frac{2}{r^2}\ ,$$

with a given by Eq. (B11).

APPENDIX C

We give here explicit expressions for $|T_{fi}|^2$ for the case wherein the nucleon-nucleon interaction in the final n-n state is included for $l\neq 0$ partial waves as well as for the s wave.

In the impulse approximation (IA), we have

$$\begin{aligned}|T_{fi}|^2\equiv\frac{4\pi}{3}\sum_{J,l}&[F_V^2|\langle j_f\|\Xi_{J,l}^{(1)}\|j_i\rangle|^2+F_A^2|\langle j_f\|\Xi_{J,l}^{(2)}\|j_i\rangle|^2\\&+(F_P^2+2F_PF_A)|\langle j_f\|\Xi_{J,l}^{(3)}\|j_i\rangle|^2-2F_VF_A\langle j_f\|\Xi_{J,l}^{(1)}\|j_i\rangle\langle j_f\|\Xi_{J,l}^{(4)}\|j_i\rangle^*\\&-2F_VF_P\langle j_f\|\Xi_{J,l}^{(3)}\|j_i\rangle\langle j_f\|\Xi_{J,l}^{(5)}\|j_i\rangle^*+F_A^2\langle j_f\|\Xi_{J,l}^{(2)}\|j_i\rangle\langle j_f\|\Xi_{J,l}^{(6)}\|j_i\rangle^*\\&+2F_PF_A\langle j_f\|\Xi_{J,l}^{(3)}\|j_i\rangle\langle j_f\|\Xi_{J,l}^{(7)}\|j_i\rangle^*]\ ,\end{aligned} \tag{C1}$$

where $|j_i=1\rangle$ is the initial deuteron state, and $|j_f\rangle$'s are final n-n states with the total spin j_f. The transition operators $\Xi_{J,l}^{(n)}$ ($n=1,\ldots,7$) are defined as below:

$$\Xi_{J,l}^{(1)}=[1-(-1)^l]j_l\left(\frac{\nu r}{2}\right)Y_l(\hat{\mathbf{r}})\delta_{J,l}\ , \tag{C2}$$

$$\Xi_{J,l}^{(2)}=j_l\left(\frac{\nu r}{2}\right)\{[Y_l(\hat{\mathbf{r}})\otimes\sigma_1]^J-(-1)^l[Y_l(\hat{\mathbf{r}})\otimes\sigma_2]^J\}\ , \tag{C3}$$

$$\begin{aligned}\Xi_{J,l}^{(3)}=&\left[\frac{l+1}{2l+1}\right]^{1/2}j_{l+1}\left(\frac{\nu r}{2}\right)\{[Y_{l+1}(\hat{\mathbf{r}})\otimes\sigma_1]^J-(-1)^l[Y_{l+1}(\hat{\mathbf{r}})\otimes\sigma_2]^J\}\delta_{J,l}\\&+\left[\frac{l}{2l+1}\right]^{1/2}j_{l-1}\left(\frac{\nu r}{2}\right)\{[Y_{l-1}(\hat{\mathbf{r}})\otimes\sigma_1]^J-(-1)^l[Y_{l-1}(\hat{\mathbf{r}})\otimes\sigma_2]^J\}\delta_{J,l}\ ,\end{aligned} \tag{C4}$$

$$\Xi_{J,l}^{(4)}=\sum_j(-1)^{j-l}\frac{\hat{j}}{\hat{l}}j_l\left(\frac{\nu r}{2}\right)(\{[Y_l(\hat{\mathbf{r}})\otimes\sigma_1]^j\otimes\mathbf{J}_d\}^J-(-1)^l\{[Y_l(\hat{\mathbf{r}})\otimes\sigma_2]^j\otimes\mathbf{J}_d\}^J)\delta_{J,l}\ , \tag{C5}$$

$$\Xi_{J,l}^{(5)}=[1+(-1)^l]\left[\left[\frac{l+1}{2l+1}\right]^{1/2}j_{l+1}\left(\frac{\nu r}{2}\right)[Y_{l+1}(\hat{\mathbf{r}})\otimes\mathbf{J}_d]^J+\left[\frac{l}{2l+1}\right]^{1/2}j_{l-1}\left(\frac{\nu r}{2}\right)[Y_{l-1}(\hat{\mathbf{r}})\otimes\mathbf{J}_d]^J\right]\delta_{J,l}\ , \tag{C6}$$

$$\Xi_{J,l}^{(6)}=\sqrt{6}\sum_j(-1)^{J+l+1}\begin{Bmatrix}l&1&J\\1&j&1\end{Bmatrix}j_l\left(\frac{\nu r}{2}\right)(\{[Y_l(\hat{\mathbf{r}})\otimes\sigma_1]^j\otimes\mathbf{J}_d\}^J-(-1)^l\{[Y_l(\hat{\mathbf{r}})\otimes\sigma_2]^j\otimes\mathbf{J}_d\}^J)\ , \tag{C7}$$

$$\Xi^{(7)}_{J,l}=\sqrt{6}\sum_j \left[\left(\frac{l+1}{2l+1} \right)^{1/2} \begin{Bmatrix} j & 1 & l \\ 1 & l+1 & 1 \end{Bmatrix} j_{l+1}\left(\frac{\nu r}{2} \right) (\{[Y_{l+1}(\hat{\mathbf{r}})\otimes\sigma_1]^j\otimes\mathbf{J}_d\}^J+(-1)^l\{[Y_{l+1}(\hat{\mathbf{r}})\otimes\sigma_2]^j\otimes\mathbf{J}_d\}^J) \right.$$
$$\left. + \left(\frac{l}{2l+1} \right)^{1/2} \begin{Bmatrix} j & 1 & l \\ 1 & l-1 & 1 \end{Bmatrix} j_{l-1}\left(\frac{\nu r}{2} \right) (\{[Y_{l-1}(\hat{\mathbf{r}})\otimes\sigma_1]^j\otimes\mathbf{J}_d\}^J+(-1)^l\{[Y_{l-1}(\hat{\mathbf{r}})\otimes\sigma_2]^j\otimes\mathbf{J}_d\}^J) \right] \delta_{J,l} , \tag{C8}$$

where $\mathbf{J}_d$ is the deuteron total spin operator.

When we include the contributions of the MEC operators described in Appendix B by making substitutions given in Eqs. (22)–(25), the expression for $|T_{fi}|^2$ becomes as follows:

$$\begin{aligned}
|T_{fi}|^2 &= 12[F_A H^0_{00}-\tfrac{1}{3}F_P(H^0_{00}+\sqrt{2}J^0_{00})]^2-8(F_A-\tfrac{1}{3}F_P)f_A\frac{1}{m_N}H^0_{00}K \\
&+\tfrac{4}{3}[F'_V(H^1_{01}-\sqrt{2}J^1_{01})-F_A(2H^1_{01}+\sqrt{2}J^1_{01})]^2 \\
&+\tfrac{4}{3}[F'_V(\sqrt{2}H^1_{11}+J^1_{11})-F_A(2\sqrt{2}H^1_{11}-J^1_{11})+F_P(\sqrt{2}H^1_{11}+J^1_{11})]^2 \\
&+\tfrac{2}{3}[F'_V(\sqrt{2}H^1_{11}+J^1_{11})-F_A(2\sqrt{2}H^1_{11}-J^1_{11})+F_P(\sqrt{2}H^1_{11}-\tfrac{4}{5}J^1_{11})]^2 \\
&+\tfrac{4}{3}[F'_V(\sqrt{2}H^1_{21}-\tfrac{1}{5}J^1_{21})-F_A(2\sqrt{2}H^1_{21}+\tfrac{1}{5}J^1_{21})]^2 \\
&+2[F'_V(\sqrt{2}H^1_{21}-\tfrac{1}{5}J^1_{21})-F_A(2\sqrt{2}H^1_{21}+\tfrac{1}{5}J^1_{21})+F_P(\sqrt{2}H^1_{21}+\tfrac{2}{5}J^1_{21})]^2 \\
&+24\left[F_A H^2_{22}-\tfrac{1}{3}F_P\left[H^2_{22}-\frac{1}{\sqrt{2}}J^2_{22}+\frac{1}{\sqrt{2}}J^0_{22}\right]\right]^2+36[F_A H^2_{22}-\tfrac{1}{3}F_P(H^2_{22}-\tfrac{1}{7}\sqrt{2}J^2_{22})]^2 \\
&+108(F_A-\tfrac{1}{3}F_P)^2(H_4)^2-\sum_{L=\text{even},L\neq 0}^{4}8(2L+1)(F_A-\tfrac{1}{3}F_P)f_A\frac{1}{m_N}H_L K_L \\
&+\sum_{L=3,5}16(2L+1)(\tfrac{1}{4}F'^2_V+F^2_A+\tfrac{1}{6}F^2_P-\tfrac{2}{3}F_P F_A-F'_V F_A+\tfrac{1}{3}F_P F'_V)(H_L)^2 \\
&-\sum_{L=\text{odd}}^{5}\tfrac{16}{3}(2L+1)(2F_A-F_P-F'_V)f_A\frac{1}{m_N}H_L K_L \\
&-8[F_A H^0_{00}-\tfrac{1}{3}F_P(H^0_{00}+\sqrt{2}J^0_{00})]\left[3D_0+\frac{m_\mu\nu}{2m_N}\frac{f_P}{f_A}(D'_0+\sqrt{2}D'_2)+\frac{\nu}{m_N}D_3\right] \\
&+\tfrac{8}{3}[F_A(H^0_{00}-2\sqrt{2}J^0_{00})+F_P(H^0_{00}+\sqrt{2}J^0_{00})]D_1 , \\
&-\tfrac{8}{9}C[F'_V(H^1_{01}-\sqrt{2}J^1_{01})-F_A(2H^1_{01}+\sqrt{2}J^1_{01})][4E^1_{01}(Y^\pi_0)+2\sqrt{2}G^1_{01}(Y^\pi_0)+2E^1_{01}(Y^\pi_2)+\sqrt{2}G^1_{01}(Y^\pi_2)] \\
&-\tfrac{4}{9}C\{2[F'_V(\sqrt{2}H^1_{11}+J^1_{11})-F_A(2\sqrt{2}H^1_{11}-J^1_{11})+F_P(\sqrt{2}H^1_{11}+J^1_{11})] \\
&\qquad+[F'_V(\sqrt{2}H^1_{11}+J^1_{11})-F_A(2\sqrt{2}H^1_{11}-J^1_{11})+F_P(\sqrt{2}H^1_{11}-\tfrac{4}{5}J^1_{11})]\} \\
&\times[4\sqrt{2}E^1_{11}(Y^\pi_0)-2G^1_{11}(Y^\pi_0)-\sqrt{2}E^1_{11}(Y^\pi_2)+14G^1_{11}(Y^\pi_2)] \\
&-\tfrac{4}{9}C\{2[F'_V(\sqrt{2}H^1_{21}-\tfrac{1}{5}J^1_{21})-F_A(2\sqrt{2}H^1_{21}+\tfrac{1}{5}J^1_{21})] \\
&\qquad+3[F'_V(\sqrt{2}H^1_{21}-\tfrac{1}{5}J^1_{21})-F_A(2\sqrt{2}H^1_{21}+\tfrac{1}{5}J^1_{21})+F_P(\sqrt{2}H^1_{21}+\tfrac{2}{5}J^1_{21})]\} \\
&\times[4\sqrt{2}E^1_{21}(Y^\pi_0)+\tfrac{2}{5}G^1_{21}(Y^\pi_0)+\tfrac{1}{5}\sqrt{2}E^1_{21}(Y^\pi_2)+\tfrac{46}{5}G^1_{21}(Y^\pi_2)] \\
&+24\sqrt{2}C\left\{2\left[F_A H^2_{22}-\tfrac{1}{3}F_P\left[H^2_{22}-\frac{1}{\sqrt{2}}J^2_{22}+\frac{1}{\sqrt{2}}J^0_{22}\right]\right]+3[F_A H^2_{22}-\tfrac{1}{3}F_P(H^2_{22}-\tfrac{1}{7}\sqrt{2}J^2_{22})]\right\}G^2_{22}(Y^\pi_2) ,
\end{aligned} \tag{C9}$$

where

$$H_{jl}^{L}=\int_0^\infty dr\frac{F_{jl}(pr)}{p}j_L\left[\frac{\nu r}{2}\right]u(r)f\left[\frac{r}{2}\right], \tag{C10}$$

$$J_{jl}^{L}=\int_0^\infty dr\frac{F_{jl}(pr)}{p}j_L\left[\frac{\nu r}{2}\right]w(r)f\left[\frac{r}{2}\right], \tag{C11}$$

$$E_{jl}^{L}(Y_i^B)=\int_0^\infty dr\frac{F_{jl}(pr)}{p}j_L\left[\frac{\nu r}{2}\right]Y_i^B(x_B)u(r)f\left[\frac{r}{2}\right], \tag{C12}$$

$$G_{jl}^{L}(Y_i^B)=\int_0^\infty dr\frac{F_{jl}(pr)}{p}j_L\left[\frac{\nu r}{2}\right]Y_i^B(x_B)w(r)f\left[\frac{r}{2}\right], \tag{C13}$$

$$C=\frac{m_\pi^3}{4\pi}\frac{4}{9}\left[\frac{f_{\pi NN^*}}{m_\pi}\right]^2\frac{f_A}{m_N^*-m_N}. \tag{C14}$$

In the above, $F_{jl}(pr)$ is the radial function for the final n-n relative motion specified by the quantum numbers $\{j,l\}$. The radial integrals K, H_L, and K_L that are concerned with the IA contributions are defined in the text [Eq. (36)], and $H_{00}^0=H$, $J_{00}^0=J$. The terms involving D_0, D_2, D_0', D_2', D_1, and D_3 are due to the MEC contributions, and their explicit expressions are given in Appendix D.

APPENDIX D

Here we deal with the two-body radial integrals D_0, D_2, D_0', D_2', D_1, and D_3 appearing in Eqs. (35) and (C9). The formalism used here essentially follows the standard procedure,[48] and we have no claim for originality in this regard. We give explicit expressions for the radial integrals just for the sake of coherence in presentation and also for clarifying the connection between the treatment of the μ-d capture and that of the ν-d reaction. The first five of the above D's are due to the axial-current MEC (Fig. 2), while D_3 is due to the vector-current MEC (Fig. 3). D_0 and D_2 arise from $\mathbf{A}^{(2)}(i,j)$ [Eqs. (22) and (B1)], D_0' and D_2' from $P^{(2)}(i,j)$ [Eqs. (23) and (B15)], and D_1 from $a^{(2)}(i,j)$ [Eqs. (25) and (B23)]. D_3 comes from $\mathbf{v}^{(2)}(i,j)$ [Eqs. (24) and (B17)]. We first give their expressions for the case wherein the form factor effects are ignored, i.e., $K_B\equiv 1$ in Eq. (26):

$$\begin{aligned}D_0=&2\sqrt{2}C_1^{(a)}J_0^2(Y_2^\pi)+\tfrac{4}{3}C_1^{(c)}\left[J_0^0(Y_0^\pi)+\frac{1}{\sqrt{2}}J_0^2(Y_2^\pi)\right]+\tfrac{4}{3}C_2^{(c)}[J_0^0(Y_0^\pi)-\sqrt{2}J_0^2(Y_2^\pi)]\\&+\tfrac{4}{3}C_1^{(d)}\left[I^0(W_1^\rho)+\frac{1}{\sqrt{2}}I^2(W_2^\rho)\right]+\tfrac{4}{3}C_2^{(d)}[I^0(W_1^\rho)-\sqrt{2}I^2(W_2^\rho)]\\&+\tfrac{4}{3}C_1^{(e)}\left[I^0(W_4^\rho)+\frac{1}{\sqrt{2}}I^2(W_5^\rho)\right]+\tfrac{4}{3}C_2^{(e)}[I^0(W_4^\rho)-\sqrt{2}I^2(W_5^\rho)]+2\sqrt{2}C_1^{(f)}J_0^2(Y_2^\rho),\end{aligned} \tag{D1}$$

$$\begin{aligned}D_2=&2\sqrt{2}C_1^{(a)}\left[J_2^0(Y_2^\pi)-\frac{1}{\sqrt{2}}J_2^2(Y_2^\pi)\right]\\&+\tfrac{4}{3}C_1^{(c)}\left[J_2^2(Y_0^\pi)+\frac{1}{\sqrt{2}}J_2^0(Y_2^\pi)-\tfrac{1}{2}J_2^2(Y_2^\pi)\right]+\tfrac{4}{3}C_2^{(c)}[J_2^2(Y_0^\pi)-\sqrt{2}J_2^0(Y_2^\pi)+J_2^2(Y_2^\pi)]\\&+\tfrac{4}{3}C_1^{(d)}\left[I^2(Z_1^\rho)+\frac{1}{\sqrt{2}}I^0(Z_2^\rho)-\tfrac{1}{2}I^2(Z_2^\rho)\right]+\tfrac{4}{3}C_2^{(d)}[I^2(Z_1^\rho)-\sqrt{2}I^0(Z_2^\rho)+I^2(Z_2^\rho)]\\&+\tfrac{4}{3}C_1^{(e)}\left[I^2(Z_4^\rho)+\frac{1}{\sqrt{2}}I^0(Z_5^\rho)-\tfrac{1}{2}I^2(Z_5^\rho)\right]+\tfrac{4}{3}C_2^{(e)}[I^2(Z_4^\rho)-\sqrt{2}I^0(Z_5^\rho)+I^2(Z_5^\rho)]\\&+2\sqrt{2}C_1^{(f)}\left[J_2^0(Y_2^\rho)-\frac{1}{\sqrt{2}}J_2^2(Y_2^\rho)\right],\end{aligned} \tag{D2}$$

$$D_0'=2\sqrt{2}C_1^{(b)}J_0^2(Y_2^\pi), \tag{D3}$$

$$D_2'=2\sqrt{2}C_1^{(b)}\left[J_2^0(Y_2^\pi)-\frac{1}{\sqrt{2}}J_2^2(Y_2^\pi)\right], \tag{D4}$$

$$D_1=2C_K^{(c)}[J_1^0(Y_1^\pi)-\sqrt{2}J_1^2(Y_1^\pi)]+2C_K^{(d)}[I^0(X_0^\rho)-\sqrt{2}I^2(X_0^\rho)]+2C_K^{(e)}[I^0(X_3^\rho)-\sqrt{2}I^2(X_3^\rho)], \tag{D5}$$

where we have used the relation $C_1^{(b)}=-C_3^{(b)}$.

$$D_3=2m_N\left[C_V^{(a)}\frac{1}{\nu}\left[J_1^0(Y_1^\pi)+\frac{1}{\sqrt{2}}J_1^2(Y_1^\pi)\right]-C_V^{(b)}\left[I^0(W_1^\pi)+I^0(Z_2^\pi)+\frac{1}{\sqrt{2}}[I^2(W_2^\pi)+I^2(Z_6^\pi)]\right]\right.$$
$$-C_V^{(c)}\left[I^0(W_1^{A_1})-I^0(Z_2^{A_1})+\frac{1}{\sqrt{2}}[I^2(W_2^{A_1})-\tfrac{1}{2}I^2(Z_7^{A_1})]\right]$$
$$\left.+C_V^{(d)}\left[\sqrt{2}J_0^2(Y_2^\pi)-J_0^0(Y_2^\pi)+\frac{1}{\sqrt{2}}J_2^2(Y_2^\pi)\right]-C_V^{(e)}\left[\sqrt{2}J_0^2(Y_2^\rho)-J_0^0(Y_2^\rho)+\frac{1}{\sqrt{2}}J_2^2(Y_2^\rho)\right]\right]. \quad \text{(D6)}$$

The integrals appearing in the above expressions are defined as follows:

$$I_0(A_l^B)=\int_0^\infty dr\frac{F_0(pr)}{p}A_l^B(r)u(r)f\left[\frac{r}{2}\right],$$
$$I^2(A_l^B)=\int_0^\infty dr\frac{F_0(pr)}{p}A_l^B(r)w(r)f\left[\frac{r}{2}\right],$$
$$J_K^0(Y_l^B)=\int_0^\infty dr\frac{F_0(pr)}{p}j_K\left[\frac{\nu r}{2}\right]Y_l^B(x_B)u(r)f\left[\frac{r}{2}\right],$$
$$J_K^2(Y_l^B)=\int_0^\infty dr\frac{F_0(pr)}{p}j_K\left[\frac{\nu r}{2}\right]Y_l^B(x_B)w(r)f\left[\frac{r}{2}\right],$$
$$W_l^B(r)=\tfrac{1}{2}\int_{-1}^{1}d\alpha\, j_0(\tfrac{1}{2}\alpha\nu r)f_l^B(r,\alpha),$$
$$X_l^B(r)=\tfrac{1}{2}\int_{-1}^{1}d\alpha\, j_1(\tfrac{1}{2}\alpha\nu r)f_l^B(r,\alpha),$$
$$Z_l^B(r)=\tfrac{1}{2}\int_{-1}^{1}d\alpha\, j_2(\tfrac{1}{2}\alpha\nu r)f_l^B(r,\alpha),$$
$$f_l^B(r,\alpha)=\exp(-a_B r)g_l^B(r,\alpha), \quad \text{(D7)}$$
$$g_0^B(r,\alpha)=1,$$
$$g_1^B(r,\alpha)=a_B-\frac{2}{r},$$
$$g_2^B(r,\alpha)=a_B+\frac{1}{r},$$
$$g_3^B(r,\alpha)=a_B^2-\frac{2}{r}a_B-\frac{2}{r^2},$$
$$g_4^B(r,\alpha)=a_B^2\left[a_B-\frac{4}{r}\right],$$
$$g_5^B(r,\alpha)=a_B^2\left[a_B-\frac{1}{r}\right]-\frac{6}{r^2}\left[a_B+\frac{1}{r}\right],$$
$$g_6^B(r,\alpha)=a_B+\frac{4}{r},$$
$$g_7^B(r,\alpha)=a_B-\frac{5}{r},$$

$$a_B\equiv a_B(m_B,m_\pi)=[\tfrac{1}{4}(1-\alpha^2)\nu^2+\tfrac{1}{2}(1+\alpha)(m_B^2-m_\pi^2)+m_\pi^2]^{1/2}. \quad \text{(D8)}$$

As discussed in the text, we take account of the finite size of N and N^* by introducing the form factor $K_B(q^2)=(\Lambda_B^2-m_B^2)/(\Lambda_B^2+q^2)$ [see Eq. (26)], where Λ_B is a cutoff factor, and m_B is the meson mass ($B=\pi$, ρ, or A_1). The introduction of $K_B(q^2)$ leads to the following transformation of the radial functions $Y_0(x_B)$, $Y_1(x_B)$, and $Y_2(x_B)$, appearing in the two-body operators:

$$Y_0(x_B)\to Y_0(x_B)-\lambda Y_0(x_\Lambda)-\frac{1}{2\lambda}(\lambda^2-1)x_\Lambda Y_0(x_\Lambda),$$
$$Y_1(x_B)\to Y_1(x_B)-\lambda^2 Y_1(x_\Lambda)-\tfrac{1}{2}(\lambda^2-1)x_\Lambda Y_0(x_\Lambda), \quad \text{(D9)}$$
$$Y_2(x_B)\to Y_2(x_B)-\lambda^3 Y_2(x_\Lambda)-\tfrac{1}{2}\lambda(\lambda^2-1)x_\Lambda Y_1(x_\Lambda),$$

with $\lambda\equiv\Lambda_B/m_B$, $x_B\equiv m_B r$ and $x_\Lambda\equiv\Lambda_B r=\lambda x_B$. Furthermore, we need to change $f_l(r,\alpha)$ in the following manner. Define

$$F_l(m_B,m_\pi)\equiv f_l^B(r,\alpha), \quad \text{(D10)}$$

and apply the modification

$$F_l(m_B,m_\pi)\to F_l(m_B,m_\pi)+F_l(\Lambda_B,\Lambda_\pi)-F_l(m_B,\Lambda_\pi)-F_l(\Lambda_B,m_\pi). \quad \text{(D11)}$$

In the present work we use the same cutoff factors for both the NNB and NN^*B vertices and choose[29]

$$\Lambda_\pi=1.25\ \text{GeV},$$
$$\Lambda_\rho=1.50\ \text{GeV}, \quad \text{(D12)}$$
$$\Lambda_{A_1}=1.85\ \text{GeV}.$$

The above explanation applies to the case of μ-d capture. In order to derive the formulas relevant to the neutrino reaction [Eqs. (40) and (50)], we only need to make the following substitutions:

$$\nu\equiv|\boldsymbol{\nu}|\to q\equiv|\mathbf{q}|,\quad f\left[\frac{r}{2}\right]\to 1. \quad \text{(D13)}$$

*Present address: The Japan Information Center of Science and Technology 2-5-2, Nagatacho, Chiyoda-ku, Tokyo 100, Japan.
†Present address: Department of Physics and Astronomy, University of South Carolina, Columbia, South Carolina 29208.

[1]F. Dautry, M. Rho, and D. O. Riska, Nucl. Phys. **A264**, 507 (1976).
[2]E. Ivanov and E. Truhlik, Nucl. Phys. **A316**, 451 (1979).

[3]I. T. Wang, Phys. Rev. **139**, B1539 (1965); M. Sotona and E. Truhlik, Nucl. Phys. **A229**, 471 (1974); G. E. Dogotar, Yu. A. Salganic, and R. A. Eramzhyan, Yad. Fiz. **22**, 472 (1975); G. E. Dogotar and R. A. Eramzhyan, *ibid.* **25**, 1042 (1977); **26**, 483 (1977); G. E. Dogotar, R. A. Eramzhyan, and E. Truhlik, Nucl. Phys. **A326**, 225 (1979); P. Pascual, R. Tarrach, and F. Vidal, Nuovo Cimento **A 12**, 241 (1972).

[4]S. Nozawa, Y. Kohyama, and K. Kubodera, Prog. Theor. Phys. **67**, 1240 (1982).

[5]B. K. Jeon, T. Sato,and H. Ohtsubo, Phys. Lett. B **228**, 304 (1989).

[6]D. O. Riska and G. E. Brown, Phys. Lett. **38B**, 193 (1972).

[7]B. Frois and C. N. Papanicolas, Annu. Rev. Nucl. Part. Sci. **37**, 133 (1987), and references therein.

[8]J. Hockert, D. O. Riska, M. Gari, and A. Huffman, Nucl. Phys. **A217**, 14 (1973); W. Leidenman and H. Arenhövel, *ibid.* **A393**, 385 (1983); J. F. Mathiot, *ibid.* **A412**, 201 (1984).

[9]J. N. Bahcall, W. G. Huebner, S. H. Lubow, and R. K. Ulrich, Rev. Mod. Phys. **54**, 767 (1982); J. N. Bahcall and R. K. Ulrich, Rev. Mod. Phys. **60**, 297 (1988).

[10]G. T. Ewan *et al.*, Sudbury Neutrino Observatory Report No. SNO-85-3, Queen's University, Canada, 1985 (unpublished); Sudbury Scientific Collaboration, Sudbury Neutrino Observatory Proposal, 1987 (unpublished); G. Aardsma *et al.*, Phys. Lett. B **194**, 321 (1987).

[11]Here and hereafter, the word "neutrino" and the symbol ν are often used rather loosely for generically referring to both the neutrino and antineutrino.

[12]G. Bardin, J. Duclos, J. Martino, A. Bertin, M. Capponi, M. Piccinini, and A. Vitale, Nucl. Phys. **A453**, 591 (1986).

[13]M. Cargnelli, dissertation, Universität Wien, 1987; M. Cargnelli, W. H. Breunlich, H. Fuhrmann, P. Kammel, J. Marton, P. Pawlek, J. Werner, J. Zmeskal, W. Bertle, and C. Petitjean, in *Proceedings of the XXIII Yamada Conference on Nuclear Weak Processes and Nuclear Structure, Osaka, 1989,* edited by M. Morita, H. Ejiri, H. Ohtsubo, and T. Sato (World Scientific, Singapore, 1989), p. 115.

[14]An estimate based on the so-called elementary-particle treatment, S. L. Mintz, Phys. Rev. C **22**, 2507 (1980), is reported to give $\lambda_d^{\text{theor}}=450\times(1\pm0.3)\ \text{s}^{-1}$, which is compatible with λ_d^{expt} of Ref. 12. This formalism, however, involves a crucial assumption on the validity of the dispersion relation applied to the weak-interaction form factors of unbound systems such as the *n-n* scattering state. Thus the reliability of the resulting estimate is expected to be much lower than the cited error indicates.

[15]S. Ellis and J. N. Bahcall, Nucl. Phys. **A114**, 636 (1968).

[16]H. C. Lee, Phys. Lett. **87B**, 18 (1979); Nucl. Phys. **A294**, 473 (1978); T. Ahrens and T. P. Lang, Phys. Rev. C **3**, 979 (1971); T. Ahrens and L. Gallaher, Phys. Rev. D **20**, 2714 (1979); A. Ali and C. A. Dominiguez, *ibid.* **12**, 3673 (1975); W. Müller and M. Gari, Phys. Lett. **102B**, 389 (1981); F. T. Avignone, Phys. Rev. D **24**, 778 (1981); J. Hosek and E. Truhlik, Phys. Rev. C **23**, 665 (1981).

[17]S. Nozawa, Y. Kohyama, T. Kaneta, and K. Kubodera, J. Phys. Soc. Jpn. **55**, 2636 (1986).

[18]J. N. Bahcall, K. Kubodera, and S. Nozawa, Phys. Rev. D **38**, 1030 (1988).

[19]Kamiokande II Collaboration, K. Hirata *et al.*, Phys. Rev. Lett. **58**, 1490 (1987).

[20]IMB Collaboration, R. M. Bionta *et al.*, Phys. Rev. Lett. **58**, 1494 (1987).

[21]E. Ivanov and E. Truhlik, Nucl. Phys. **A316**, 437 (1979).

[22]H. Primakoff, Rev. Mod. Phys. **31**, 802 (1959); A. Fujii and H. Primakoff, Nuovo Cimento **12**, 327 (1959); R. J. Blin-Stoyle, *Fundamental Interactions and the Nucleus* (North-Holland, Amsterdam, 1973).

[23]E. Klemt, P. Bopp, L. Hornig, J. Last, S. J. Freedman, D. Dubbers, and O. Schärpf, Z. Phys. C **37**, 179 (1988); L. H. Chan, K. W. Chen, J. R. Dunning, Jr., N. F. Ramsey, J. K. Walker, and R. Wilson, Phys. Rev. **141**, 1298 (1966); E. B. Hughes, T. A. Griffy, M. R. Yearian, and R. Hofstadter, *ibid.* **139**, B458 (1965).

[24]Particle Data Group, Phys. Lett. **170B**, 1 (1986).

[25]V. I. Ogievetsky and B. M. Zupnik, Nucl. Phys. **B24**, 612 (1970).

[26]M. Chemtob and M. Rho, Nucl. Phys. **A163**, 1 (1971).

[27]K. Kubodera, J. Delorme, and M. Rho, Phys. Rev. Lett. **40**, 755 (1978).

[28]M. Doi, T. Sato, H. Ohtsubo, and M. Morita, Nucl. Phys. **A511**, 507 (1990); (private communication).

[29]E. Truhlik and J. Adam, Jr., Nucl. Phys. **A492**, 529 (1989).

[30]R. V. Reid, Jr., Ann. Phys. (N.Y.) **50**, 411 (1968).

[31]M. Lacombe, B. Loiseau, J. M. Richard, R. Vinh Mau, J. Côté, P. Pirès, and R. de Tourreil, Phys. Rev. C **21**, 861 (1980).

[32]A. J. F. Siegert, Phys. Rev. **52**, 762 (1937).

[33]J. L. Friar and S. Fallieros, Phys. Rev. C **13**, 2571 (1976); Phys. Lett. **114B**, 408 (1982); Phys. Rev. C **29**, 1645 (1984); F. Partovi, *ibid.* **36**, 491 (1987).

[34]S. Ying, E. M. Henley, and G. A. Miller, Phys. Rev. C **38**, 1584 (1988).

[35]For a review, L. Grenacs, Annu. Rev. Nucl. Part. Sci. **35**, 455 (1985).

[36]M. Oka and K. Kubodera, Phys. Lett. **90B**, 45 (1980).

[37]For example, N. C. Mukhopadhyay, Phys. Rep. **30**, 1 (1977).

[38]L. A. Ahrens *et al.*, Phys. Lett. B **202**, 284 (1988).

[39]H. H. Chen, Phys. Rev. Lett. **55**, 1534 (1985); R. S. Raghavan, S. S. Pakvasa, and B. A. Brown, Phys. Rev. Lett. **57**, 1801 (1986); S. Weinberg, Int. J. Mod. Phys. A **2**, 301 (1987).

[40]S. P. Mikheyev and A. Yu. Smirnov, Nuovo Cimento C **9**, 17 (1986); L. Wolfenstein, Phys. Rev. D **17**, 2369 (1978).

[41]The cross section obtained in the elementary-particle treatment, S. L. Mintz, Phys. Rev. D **22**, 2918 (1980), is significantly larger than the value obtained in the standard IA-plus-exchange-current approach used here. As discussed in Ref. 14, however, the reliability of the elementary-particle approach in the present case is not established.

[42]In the present work we have retained the q^2 dependence of the nucleon weak-interaction form factors, whereas the previous works (Refs. 1 and 2) used the form factors at the fixed momentum transfer $q^2=0.89m_\mu^2$, corresponding to the formation of the final *n-n* system with no internal energy. We have found that the use of the "fixed-q^2 approximation" changes λ_d by less than 1%.

[43]J. N. Bahcall and B. R. Holstein, Phys. Rev. C **33**, 2121 (1986).

[44]J. R. Wilson, in *Numerical Astrophysics,* edited by J. Cantrella *et al.* (Jones & Bartlett, Boston, 1986), p. 422; H. A. Bethe, G. E. Brown, J. Applegate, and J. M. Lattimer, Nucl. Phys. **A324**, 487 (1979); A. Burrows and J. M. Lattimer, Astrophys. J. **295**, 14 (1985); J. R. Wilson, R. Mayle, S. E. Woosley, and T. E. Weaver, Ann. N.Y. Acad. Sci. **470**, 267 (1986); J. N. Bahcall, A. Dar, and T. Piran, Nature (London) **326**, 135 (1987); J. N. Bahcall, T. Piran, W. H. Press, and D. N. Spergel, *ibid.* **327**, 682 (1987).

[45]After the completion of this paper, we have come to know the existence of a similar work by the University of Washington

group: S. Ying, W. C. Haxton, and E. M. Henley, Phys. Rev. D **40**, 3211 (1989).

[46]After the submision of the present article, the following detailed study of the μ-d capture was brought to our attention: J. Adam, Jr., E. Truhlik, S. Ciechanowicz, and K.-M. Schmitt, Nucl. Phys. **A507**, 675 (1990).

[47]O. Schori, B. Gabioud, C. Joseph, J. P. Perroud, D. Rüegger, M. T. Tran, P. Truöl, E. Winkelmann, and W. Dahme, Phys. Rev. C **35**, 2252 (1987), and references therein.

[48]For the detailed description of a similar treatment of the electromagnetic processes, see Ref. 29 and references therein. For a consistent formalism for taking into account the effects of the form factors appearing in the meson-nucleon and current-nucleon couplings, see F. Gross and D. O. Riska, Phys. Rev. C **36**, 1928 (1987).